



Spatial variability of Fe and Mn in surface lake sediments and its implications for paleoredox studies – a case study of Lake Łazduny (Poland)

Maurycy Żarczyński¹, Dirk Enters^{2,3}, Beata Szymczycha⁴, Wojciech Tylmann¹

5 ¹Department of Geomorphology and Quaternary Geology, Faculty of Oceanography and Geography, University of Gdańsk, Gdańsk, 80309, Poland

²Lower Saxony Institute for Historical Coastal Research, Wilhelmshaven, 26382, Germany

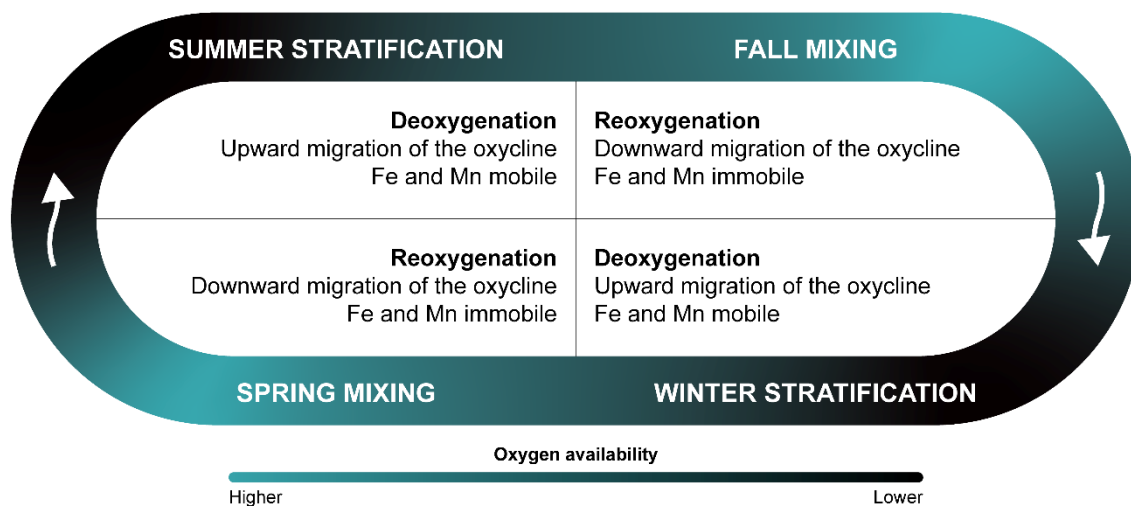
³Institute of Geography, University of Bremen, Bremen, 28359, Germany

10 ⁴Department of Marine Chemistry and Biochemistry, Institute of Oceanology of the Polish Academy of Sciences, Sopot, 81712, Poland

Correspondence to: Maurycy Żarczyński (maurycy.zarczynski@ug.edu.pl)

Abstract. Numerous lakes worldwide are deteriorating due to climate change and other human impacts. Specifically, low dissolved oxygen levels are threatening food webs and water security. Protection, mitigation, and future projections of these phenomena call for a better understanding of their past evolution. For decades, paleolimnology has provided information about past environments by studying sediment structure and geochemistry. Among the latter, iron (Fe) and manganese (Mn), and their ratios are well-established proxies of the past water oxygenation. However, the understanding of redox-sensitive elements' mobility calls for a still scarce use of spatial approaches, complementing typical investigations focused on temporal geochemical variability. To address that, we began with 33-month-long observations of limnological conditions (water temperature and dissolved oxygen concentration) in a small, deep lake experiencing seasonal anoxia, continued with characterization of major sediment structures, and concluded with geochemical and statistical analyses of collected material. We used 31 surface samples from different depths and investigated their sediment structures, bulk geochemistry (CNS and biogenic silica), elemental composition (micro-X-ray fluorescence), and Fe and Mn fractions. Our data indicate clear, testable links between oxygen availability and sediment structures, as well as their chemical composition. Anoxia promotes the deposition and preservation of laminations. Whereas seasonally migrating oxycline drives geochemical focusing, enriching the deepest sediments in Fe and Mn. This proves that both Fe and Mn are reliable indicators of deep-water redox conditions. Our study bridges modern limnology and paleolimnology and emphasizes the need to treat lakes and their sediments as a complete, complex system.

15
20
25



1 Introduction

30 Rapidly accelerating environmental changes, intensified by anthropogenic activities, are exerting profound impacts on ecosystems worldwide. One of the most vulnerable environments are inland waterbodies, providing water security, sustenance, and many other ecosystem services (Peterson et al., 2003). Lakes are intricate systems inseparable from the atmosphere, lithosphere, and biosphere, where multiple processes form complex loops. Among the most critical parameters affecting lakes is the availability of dissolved oxygen (DO) (Wetzel, 2001), as it is crucial for the respiration and transformation of matter within the lake. Rising temperatures, a shift towards eutrophic conditions, and pollution affect lakes worldwide (Jane et al., 2021; Jenny et al., 2016b). Importantly, rising temperatures reduce dissolved oxygen (DO) concentrations in aquatic systems due to decreasing gas solubility with increasing water temperature and by stronger water column stratification. Numerous studies have investigated DO dynamics with respect to climate change and eutrophication (Dresti et al., 2022; Hounshell et al., 2021; Li et al., 2018; Yuan and Jones, 2020). These processes have been accelerating in the “Anthropocene“ (Poraj-Górska et al., 2021) as hypoxia spreads and mixing regimes change (Jenny et al., 2016a; Woolway and Merchant, 2019). Countermeasures and treatments for hypoxia require an understanding of the past and present processes driving water deoxygenation.

Geological records such as lake sediments provide means to reconstruct past changes in water oxygenation (Naeher et al., 2013), as redox conditions influence the behavior of certain elements and compounds. Thus, geochemical variability traces past redox conditions at the time of sediment formation, as well as those that persisted during early diagenesis. Iron (Fe) and manganese (Mn) are well-established elements used in paleoredox studies because their mobility depends on the oxidation state and burial conditions (Engstrom and Wright, 1984; Mackereth, 1966). Typically, paleolimnologists investigate sediments retrieved from a single location of a specific lake. Studies investigating Fe and Mn in multiple cores from one site



are still scarce (Scholtysik et al., 2020; Sirota et al., 2024). Yet, Fe and Mn mobility and deposition are also influenced by
50 supply rates and biogeochemical cycles involving, but not limited to, the mineralization of organic matter (He et al., 2023;
Vegas-Vilarrúbia et al., 2018; Żarczyński et al., 2019). Relationships among sediment sources, lake morphology, and water
properties can lead to geochemical focusing, the transport of redox-sensitive elements along depth gradients, and their
deposition in local depressions of lakes and marine basins. Therefore, the interpretation of any paleoredox signal is not
straightforward, and studies using more than one sediment core are an invaluable source of information (Engstrom et al.,
55 1985).

To understand the potential of Fe and Mn as paleoredox proxies, it is necessary to recognize their spatial extent and mobility
within the lakes. Specifically, the position and depth of the sampling site could influence the interpretation of the paleoredox
signal with respect to possible Fe and Mn fate within the sediments, where either enrichment or depletion of these elements
is linked to whole-lake oxygen conditions (Scholtysik et al., 2020; Sirota et al., 2024). This study uses surface sediment
60 samples from Lake Łazduny in north-eastern Poland to examine relationships between Fe and Mn abundances and the spatial
diversity of bottom-water oxygen availability, thereby improving understanding of the fundamental roles of Fe and Mn in
paleoredox studies. The presence of annual lamination (varves) and limnological data indicate that the lake water is
seasonally stratified with recurring hypolimnetic hypoxia (Zolitschka et al., 2015). This lake has been studied intensively
over the last decade, offering a rich background on the limnological and hydrochemical properties of the water column
65 (Sanchini et al., 2020; Szczerba et al., 2023; Tylmann et al., 2013b, 2017). Clear patterns of Fe and Mn make it an excellent
site for studying the relationships between water-column dynamics and sedimentation processes.

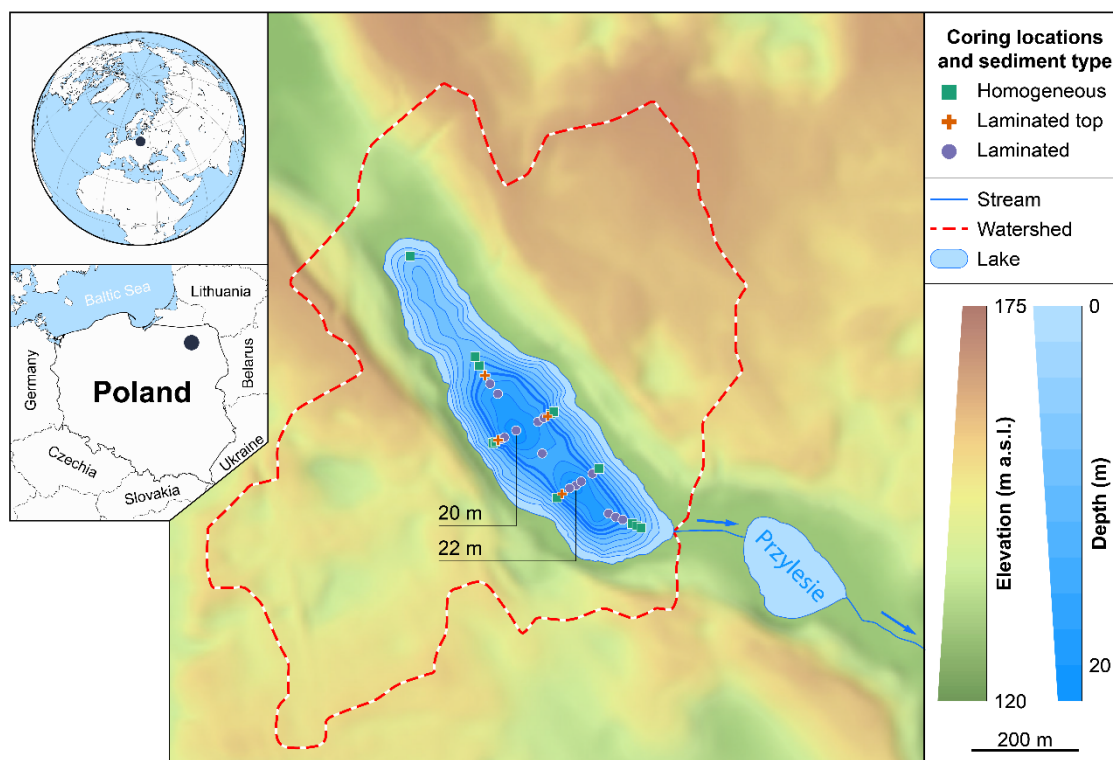
We hypothesize that the lithology and composition of surface sediments reflect the dynamics of recent lake mixing and
oxygen availability. In Lake Łazduny, oxygen-driven changes of Fe and Mn mobility lead to geochemical focusing and
downslope migration of Fe and Mn. Therefore, higher concentrations of these metals indicate seasonal shifts between oxic
70 and anoxic conditions in the water column. This flickering in oxygen availability is a mechanism responsible for the final
fate of Fe and Mn. To test this hypothesis, we aim to 1) characterize water column physicochemical parameters, mixing
dynamics, and oxygen availability; 2) compare spatial variability of the sediment structure and selected geochemical
variables with the typical bottom water oxygenation conditions; and 3) test whether Fe and Mn concentrations are
statistically different in homogeneous and laminated sediment sections.

75 **2 Study site**

Lake Łazduny is a small (0.11 km²; 53°51'18" N, 21°57'07" E; 129 m a.s.l.), moderately deep, endorheic basin divided by a
sill into two basins of 20 and 22 m depth (Fig. 1). It is a hardwater, mesotrophic water body occupying a tunnel channel in
the Masurian Lakeland (NE Poland), which was cut into outwash sands and gravels of the Pomeranian phase of the Vistulian
glaciation, ca. 16–17 ka BP (Marks et al., 2016). Charophyta meadows occupy the littoral zone. The region's mean annual
80 temperature is approximately 8.0 °C (January: -2.5 °C, July: 18.5 °C), and the mean annual precipitation is approximately



600 mm (1991–2020; Tomczyk and Bednorz, 2022). Westerly and south-westerly winds are predominant in the Masurian Lakeland (Hutorowicz et al., 1996). Ongoing limnological observations indicate a seasonally stratified water column with an anoxic hypolimnion (Szczërba et al., 2021). A complete lake turnover (holomixis) can occur once or twice per year, depending on the weather conditions. These events in spring and fall temporarily reoxygenate deep waters. However, DO is rapidly utilized by biogeochemical processes at the sediment-water interface. In some years, however, rapid stratification in spring or ice cover in late fall prevents holomixis.



90 **Figure 1:** Location of Lake Łazduny, digital elevation model (LIDAR data courtesy of the Polish Head Office of Geodesy and Cartography), and lake bathymetry. Coring locations and sediment types are indicated with colored symbols. Isobaths at 12 m and 14 m are thicker and depict approximate extent of the predominantly hypoxic and anoxic zones.

3 Material and methods

3.1 Limnological monitoring, coring, and sampling

Water temperature and dissolved oxygen concentration were measured monthly from October 2007 to August 2010 at 1-m intervals over the northern deep point using a YSI 6820 Multiparameter sonde (YSI). Thirty-one sediment cores, LAZ–10/01 to LAZ–10/31, up to 96 cm long, were collected in 2010 with a gravity corer (Tylmann, 2007) equipped with a 60 mm diameter PVC tubes at a regular depth interval (Fig. 1). Retrieved cores were tightly sealed and transported to the GEOPOLAR laboratory (University of Bremen, Germany) and stored at a temperature of 4 °C. Afterwards, cores were split



lengthwise, described macroscopically and photographed. Finally, samples from the top 1 cm of each core were taken, dried, and homogenized in an agate mortar.

100 **3.2 Elemental analysis and non-destructive μ XRF scanning**

For elemental (CNS) analysis of total carbon (TC), total nitrogen (TN), and total sulfur (TS), homogenized sediment samples were weighed into tin (Sn) capsules with tungsten trioxide (WO_3) catalyst. To analyze total organic carbon (TOC), a second batch of sediments was weighed into silver (Ag) capsules, heated to 80 °C, and acidified with 3% and 20% HCl to remove carbonates. The capsules were then rinsed with distilled water. Concentrations of TC, TN, and TS were determined with the
105 EuroEA elemental analyzer (Eurovector). Total inorganic carbon (TIC) was calculated by subtracting TOC from TC. Biogenic silica (BSi) concentrations were determined after sample digestion in 1 mol NaOH at 70 °C using a segmented flow procedure (Müller and Schneider, 1993).

A non-destructive micro-X-ray fluorescence (μ XRF) scan was performed with an ITRAX core scanner (Cox Analytical Systems) at the GEOPOLAR. Samples were fixed in an acrylic glass sample carrier (Ohlendorf, 2018) and scanned using a
110 molybdenum (Mo) X-ray source (30 kV, 25 mA), with a 100 s count time per sample. Due to the compositional nature of μ XRF data, results were converted to centered log-ratios (clr) (Bertrand et al., 2024).

3.3 Fe and Mn sequential extraction

A four-step sequential extraction of Fe and Mn fractions was performed following the procedure of Tessier et al. (1979) and Zimmerman and Weindorf (2010). Solutions of surface-bound ions, (oxy)hydroxides, organic matter-bound ions, and ions
115 within the siliciclastic minerals' lattices were measured using an atomic absorption spectrometer AA-6800 (Shimadzu) at the Institute of Oceanology, Polish Academy of Sciences (Sopot). A detailed procedure is available in the Appendix.

3.4 Statistical analysis

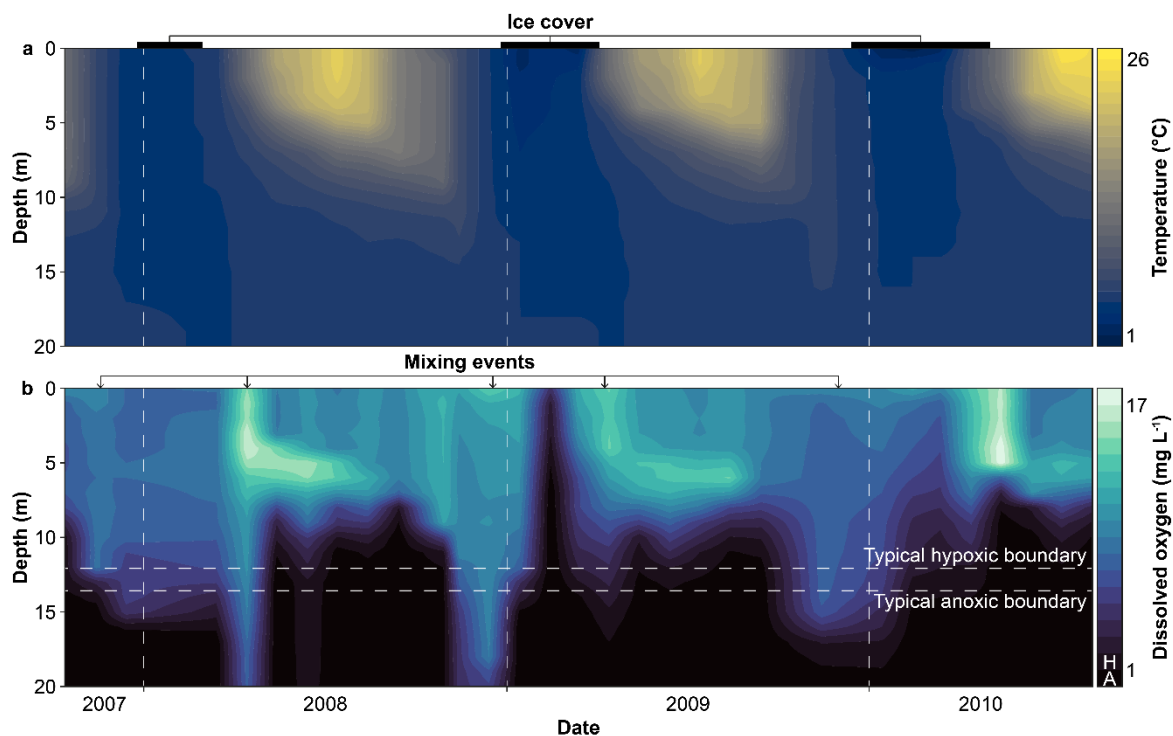
All statistical procedures were conducted using R 4.5.1 (R Core Team, 2025). To achieve a better balance between groups, partially laminated and homogeneous sediments were aggregated. The “tidyverse” 2.0.0 (Wickham et al., 2019) was used for
120 most of the analyses and visualization. μ XRF data were processed using the “robCompositions” 2.4.1 (Templ et al., 2011). Due to the non-normal distribution of analyzed variables, Spearman's rank correlation was used to test relationships between the proxies. A robust principal component analysis (RPCA) was used to visualize the overall data structure and internal relationships between the variables using the “pcaPP” 2.0-5 (Filzmoser et al., 2024). Before the multivariate statistics, data were log-transformed, scaled, and centered. Spatial interpolation was performed using the thin plate spline regression with
125 “fields” 16.3.1 (Nychka and Furrer, 2021). To test whether there are significant differences between the selected variables and between the sediment classes, we used a non-parametric Wilcoxon test. Generalized additive models (GAMs) were fitted using “mgcv” 1.9-3 (Wood, 2019).



4 Results

4.1 Limnological observations

130 Lake Łazduny water temperature exhibited seasonal stratification and homothermy typical of temperate-climate zone lakes in central Europe (Fig. 2a). Brief mixing in spring and fall separated the summer and winter stratification periods. The maximum surface water temperature reached 26.1 °C in July 2007. Under the ice, reverse stratification was typical but relatively weak, closer to homothermic conditions, and occurred shortly during the lake turnovers. The ice onset was stable, beginning in December, while the thaw depended on the spring temperatures. The ice cover lasted between 66 and 140 days, breaking up between early March (2008) and early May (2010). Oxygen concentrations during the study period varied with time and depth (Fig. 2b). The depth of the oxycline shifted between 6 m and 20 m (complete turnover). On average, the boundary of hypoxic conditions (< 2 mg L⁻¹ DO) resided around the depth of 12 m, while anoxic conditions (< 1 mg L⁻¹ DO) established between 13 and 14 m deep (oxygen levels follow Nürnberg, 1995). Surface waters remained oxygenated. The highest oxygen concentrations were observed at 5–6 m, reaching 17.9 mg L⁻¹. In January 2009, under the ice cover, extremely low DO concentrations developed throughout the majority of water column, with only the first 5 meters remaining oxygenated. Two complete turnovers were registered in Lake Łazduny during the study period, temporarily reoxygenating the hypolimnion. Mixing events began with an oxycline near the water's surface, which then migrated downward, occasionally reaching the sediments. Typically, less than 30 days were necessary for oxygen consumption and reestablishment of anoxia. During the stratification period, the oxycline migrated upwards.



145



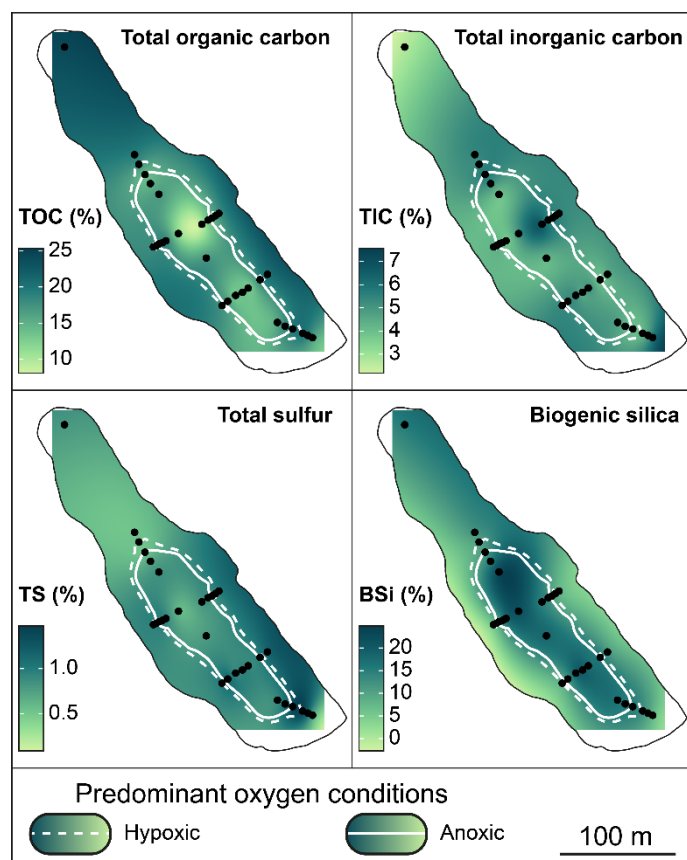
Figure 2: Lake Łazduny water properties based on *in situ* measurements between October 2007 and August 2010: (a) water temperature and (b) dissolved oxygen concentration. Black horizontal bars indicate ice cover.

4.2 Sediment structure

The structure of the surface sediments in Lake Łazduny varied with distance from the shoreline and depth (Fig. 1), as well as with average oxygen availability. Homogeneous sediments were located closest to the lake shore at depths up to 12 m, where oxic conditions prevailed. Partially laminated sediments occupied a transition zone between 12 and 15 m, experiencing a migrating oxycline. The depth of this gradual change in sediment structure corresponds to the average depth of the anoxic/hypoxic boundary. Below 15 m, underneath the predominantly anoxic hypolimnion, only laminated sediments occurred.

155 4.3 Bulk CNS and biogenic silica

Elemental data varied depending on the location (Fig. 3, Tab. A1). Organic matter, represented by TOC (5.5%–24.3%), was deposited mainly in the oxic littoral zone. Additionally, the northern part of the lake is dominated by *Chara*, which increases the abundance of aquatic organic matter (low C/N, Fig. A1). The western and south-western littoral is enriched with terrestrial organic matter originating from the catchment (higher C/N, Fig. A1). The central, anoxic part of the basin, where laminated sediments were found, was depleted in organic matter. The difference between homogeneous and laminated sediments is significant ($W = 101, p < 0.05$). Concentrations of TIC (2.4%–8.3%), representing the carbonates, were typically higher in the oxic zone. Mean TIC concentrations were higher in the homogeneous sediments and lower concentrations in the laminated sediments were statistically different ($W = 85, p < 0.5$). Total sulfur concentrations (0.2%–1.6%) were the highest close to the shores and outlet on the southern end. However, generally, TS exhibited a more random pattern. There was no substantial difference between mean concentrations of the massive and laminated sediments ($W = 112, p > 0.5$). Biogenic silica, a primary production proxy representing the deposition of siliceous algae such as diatoms, showed a deposition pattern that was somewhat opposite to that of TOC. The highest concentrations were found in the anoxic, laminated sediments (max = 25.2%). In contrast, in the shallow, oxic, homogeneous sediments, concentrations were significantly lower ($W = 217, p < 0.5$).



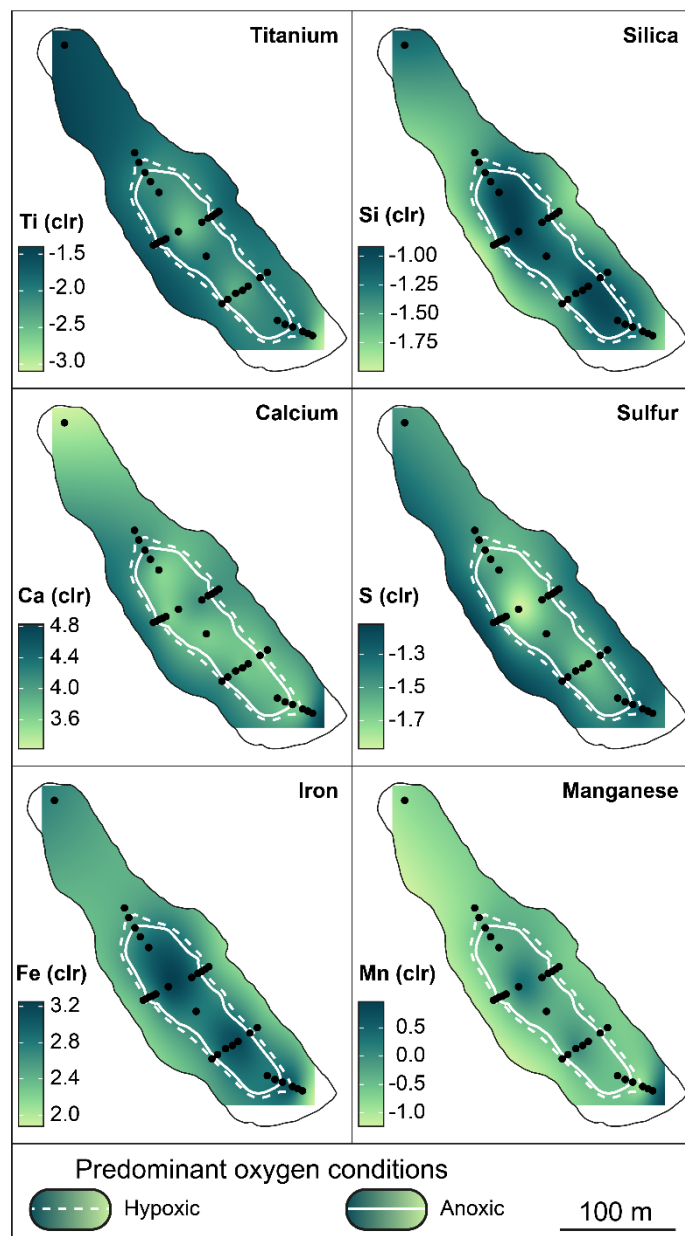
170

Figure 3: Spatial variability of selected elemental variables. Dots indicate coring locations.

4.4 μ XRF elemental geochemistry

μ XRF data (Fig. 4) showed similar trends to those of elemental data (Fig. 3). Titanium (Ti_{clr}), a terrigenous input proxy concentrated in the littoral zone, with the lowest values in the deep basins. Sulfur (S_{clr}) showed a similar pattern to TS, and it was primarily depleted in the deep sediments. Despite its expected detrital origin, silica (Si_{clr}) showed deposition patterns comparable to those of BSi (Figs. 3 and 4), with the highest concentrations in the lake's deepest, anoxic parts. Calcium (Ca_{clr}) was mainly associated with TIC concentrations. Finally, redox-sensitive iron (Fe_{clr}) and manganese (Mn_{clr}) showed enrichment in the deepest, anoxic parts of the lake, with an overall pattern opposite to that of sulfur. Si_{clr} , Fe_{clr} , and Mn_{clr} exhibited a sharp increase with depth and the spatial extent of anoxia.

175



180

Figure 4: Spatial variability of selected elements from the μ XRF scan. Dots indicate coring locations.

4.5 Iron and manganese fractionation

The distribution of four major Fe fractions is shown in Figure 6. Overall, in agreement with μ XRF data, most Fe was concentrated in the deepest, anoxic parts of the lake (Tab. A2). The total concentration of Fe (Fe_{tot}) in the laminated sediments differed significantly and was greater than in the homogeneous sediments ($W = 185, p < 0.05$). The mean concentration in the laminated sediments reached $9649.93 \mu\text{g g}^{-1}$, whereas in the homogeneous sediments it was $6020.25 \mu\text{g}$

185



190 g^{-1} . Fe_{tot} was highly correlated with the Fe_{clr} record ($\rho = 0.92$, Fig. A2). Especially surface-bound ions (Fe_{surf}) and Fe (III) (oxy)hydroxides (Fe_{oxy}) showed enrichment in the deepest parts of the lake. Fe ions bound to the organic matter (Fe_{org}) exhibited similar patterns to those of TOC (Fig. 3). Finally, ions bound within the crystal lattice of siliciclastic minerals (Fe_{sili}), showed distribution like Fe_{surf} and Fe_{oxy} , with the highest concentrations found in laminated sediments (Fig. 5). However, there was a noticeable shift towards the western littoral zone compared to Fe_{oxy} .

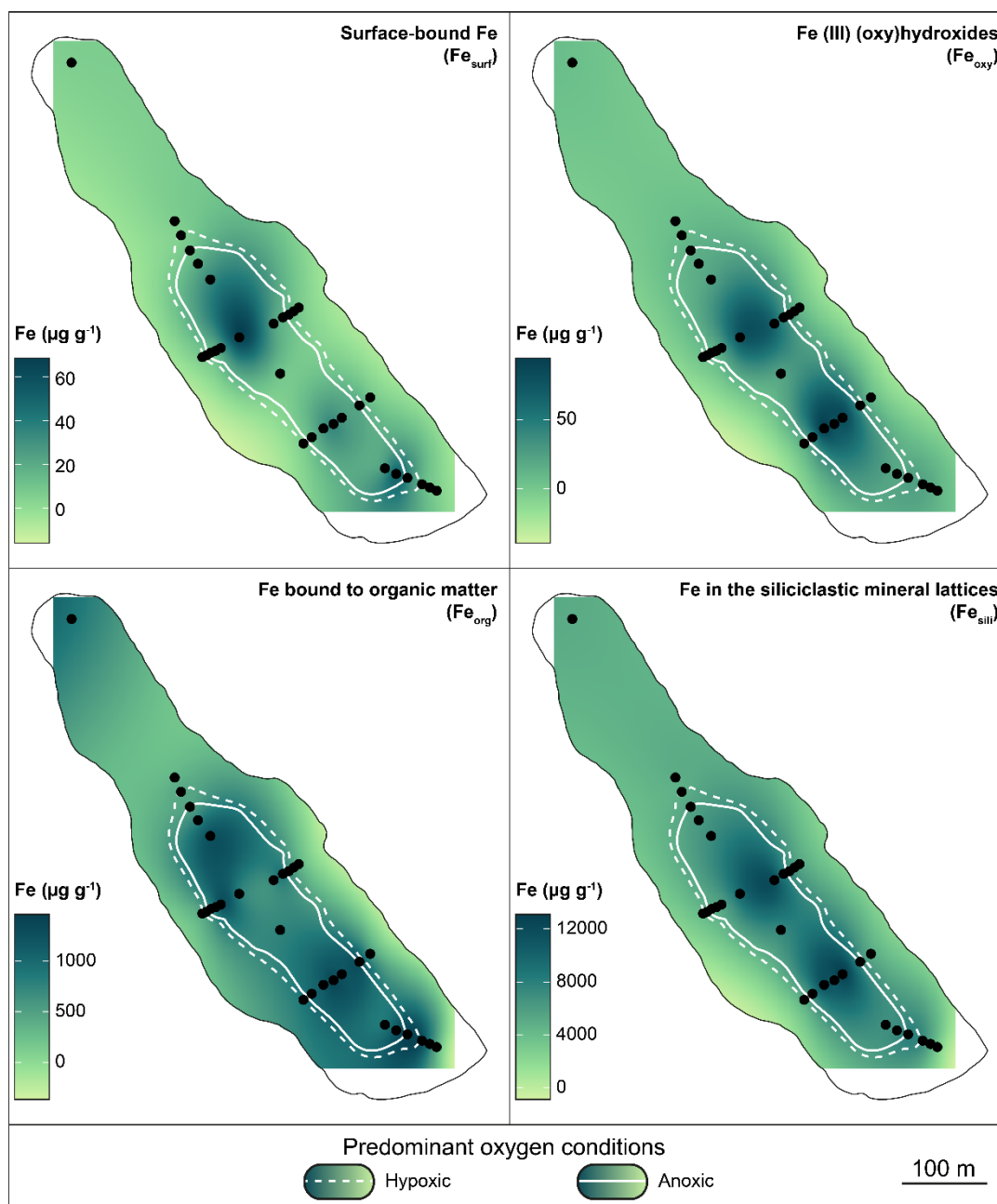




Figure 5: Spatial variability of Fe fractions in the sediments. Dots indicate coring locations.

195 Similarly, four Mn fractions were studied (Fig. 6, Tab. A3). The highest total Mn (Mn_{tot}) concentrations were observed in the central, anoxic part of the lake (Fig. 6), averaging $556.4 \mu\text{g g}^{-1}$. In contrast, in the homogeneous sediments, Mn_{tot} averaged at $369.3 \mu\text{g g}^{-1}$ (Tab. A3). Like the Fe_{tot} concentrations, Mn_{tot} concentrations were higher in the laminated sediments than in the homogeneous sediments ($W = 157.5$, $p < 0.05$). Mn_{tot} was highly correlated with the Mn_{clr} ($\rho = 0.96$, Fig. A2). Surface-bound ions (Mn_{surf}) were abundant in the central part of the basin, while the shallow northern part and lake shoreline were depleted. Mn (IV) (oxy)hydroxides (Mn_{oxy}) showed the most striking spatial pattern and were most abundant in the deepest parts of the lake (Fig. 6). Mn bound to organic matter (Mn_{org}) was enriched in the deepest parts of the lake. Mn within a crystal lattice of siliciclastic minerals (Mn_{sili}) once again showed enrichment in the deepest part of the lake. However, similarly to the Fe_{sili} , it was slightly shifted towards the western shore of the lake in comparison to Mn_{oxy} .

200

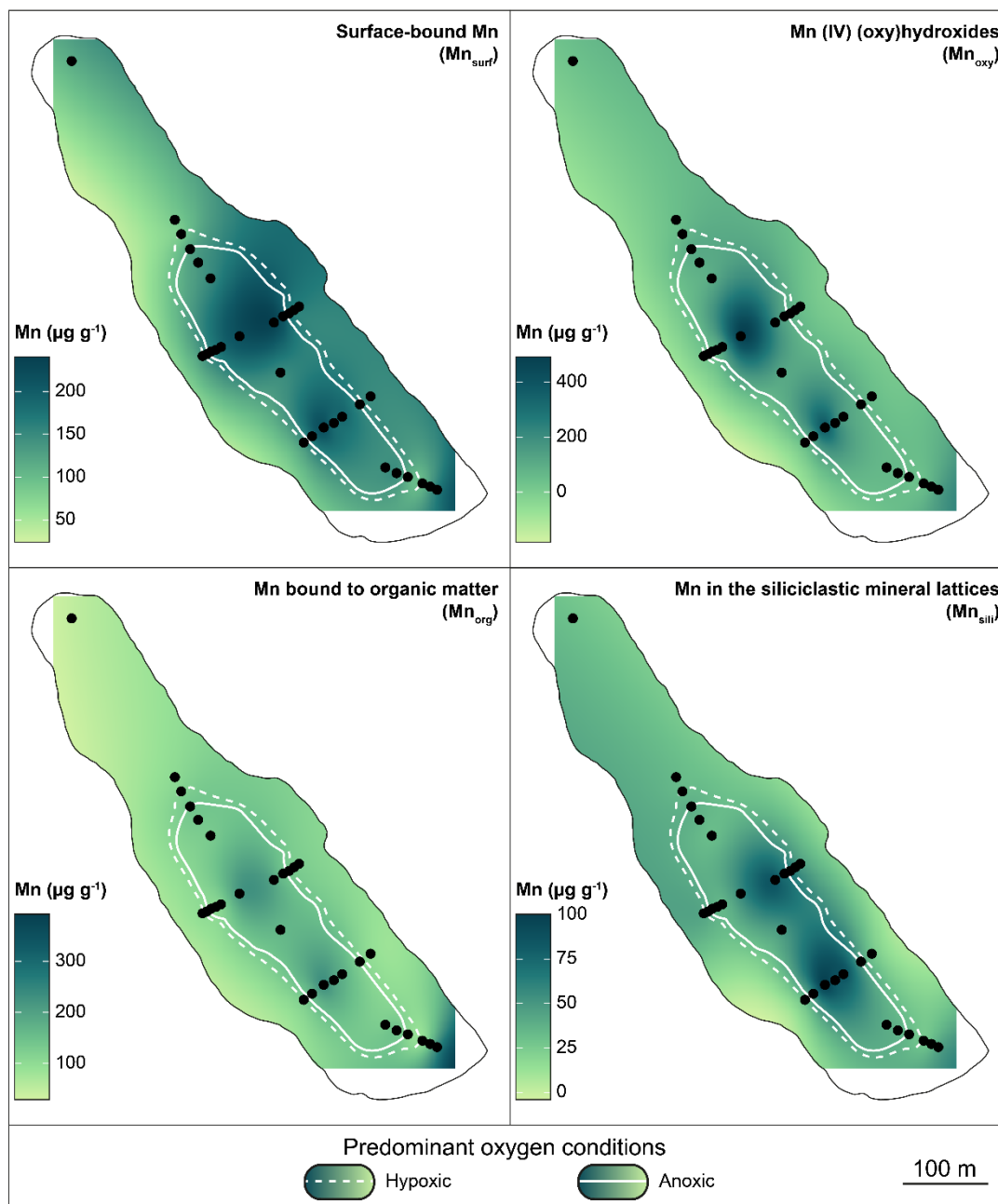


Figure 6: Spatial variability of Mn fractions in the sediments. Dots indicate coring locations.

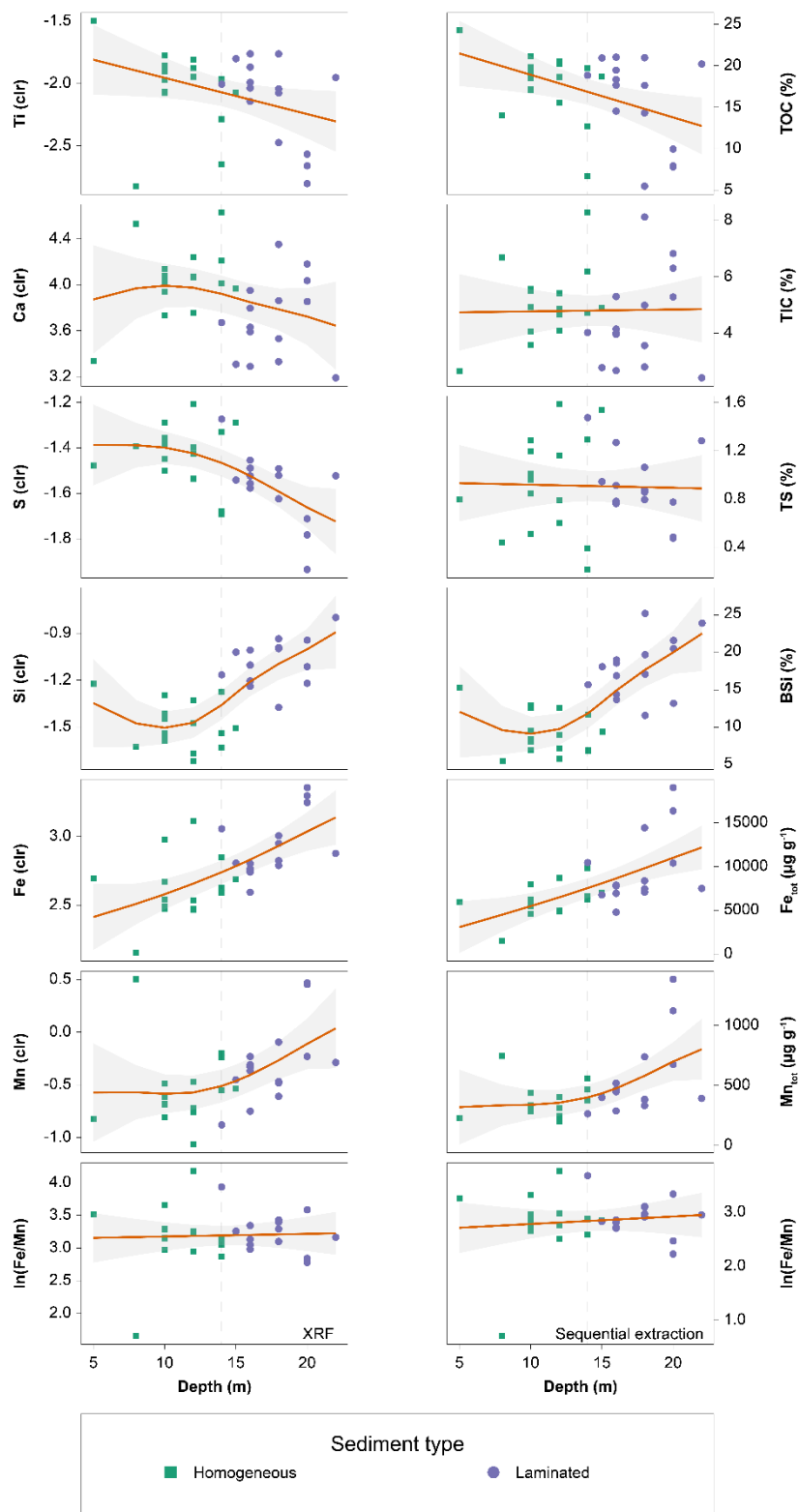
205 4.6 Statistical relationships

Relationships between the sampling depth, sediment type, oxygen conditions, and selected geochemical variables are shown in Figures 7 and A4. Ti_{clr} and TOC behaved similarly, showing lower values with increasing depth and anoxia. The second group of elemental variables, Ca_{clr} and TIC, showed flat slopes and were influenced by outliers, with no clear separation



210 between the oxidation zones. S_{clr} and TS showed a weak tendency towards lower values with increasing depth. A comparison between the Si_{clr} and BSi datasets showed agreement, indicating enrichment with depth and a baseline shift within the anoxic zone.

215 Fe_{clr} and Fe_{tot} had an almost linear relationship with the increasing depth (Fig. 7), with a clear separation between the homogeneous and laminated sediments and the oxic and anoxic zones (Fig. 5 and 7, Fig. A3 and A4). The response of the Mn_{clr} and Mn_{tot} to the depth increase was weaker (Fig. 7). Relations were non-linear, and the separation in intermediate depths was not as straightforward as Fe. The lowest concentrations were associated with homogeneous sediments, while the highest were associated with laminated sediments. Fe/Mn ratios, based on μXRF and sequential extraction, showed good agreement (Fig. A5, Fig. 7). Generally, the ratio exhibited a weak yet expected tendency towards higher values in the deeper lake zones. However, there were some outliers.





220 **Figure 7: Change in measured element abundances, concentrations, and ratios with sediment depth. GAMs are shown as smooth lines with a 0.95 confidence interval.**

5 Discussion

5.1 Limnological regime and sediment lithology

Figure 8 depicts the expected behavior of the Lake Łazduny water column, dissolved and particulate matter, and sediments
225 in response to changing limnological conditions. Lake Łazduny exhibits a limnological regime like that of other temperate-
climate lakes. The defining features are seasonal thermal stratification and spring and fall turnovers (Bonk et al., 2015;
Roeser et al., 2021). Depending on the meteorological conditions, Lake Łazduny shifts between dimictic, monomictic, and
meromictic mixing regimes (Szczerba et al., 2021). Even in deep lakes short and intense mixing events occasionally
reoxygenate the hypolimnion (Żarczyński et al., 2022). Sedimentation in Lake Łazduny follows the well-described pattern
230 observed in other lakes with varved sediments (Zolitschka et al., 2015) with diagnostic calcite laminations (Tylmann et al.,
2013a). During the warm season, increased primary production and higher water temperatures influence the epilimnetic pH
and carbon budget, steering carbonate precipitation (Dean and Megard, 1993).

After stratification onset, oxygen in the deep water is rapidly consumed, leading to anoxia. Depending on
hydrometeorological conditions and ice phenology, the bottom waters of Lake Łazduny can remain anoxic for extended
235 periods, spanning multiple years (Szczerba et al., 2021). Thus, the water column is separated into the mixolimnion and the
monimolimnion (Boehrer et al., 2017). Each year as the oxycline moves downward, a portion of the lake bottom reaching at
times up to 14–15 m deep is oxidized (Fig. 8). Conversely, once stratification develops, the oxycline moves back toward the
surface, and the lakebed area under anoxic conditions extends. Oxygen conditions control post-depositional sediment
stability as laminations are easily destroyed by bioturbation and gas release. In the absence of oxygen, these processes are
240 restricted, allowing varve preservation (Zolitschka et al., 2015).

The spatial diversity of the sediment lithology in Lake Łazduny corresponds to the average extent of hypoxic and anoxic
conditions. This resembles Lake Suminko, where Tylmann et al. (2012) demonstrated that the spatial extent of the varved
sediments mirrors the extent of the monimolimnion. In Lake Łazduny, homogeneous sediments occupy parts of the lake
subject to intense mixing and permanent oxic conditions. The deeper transition zone (≈ 12 –14 m depth), which is at least
245 seasonally hypoxic, is characterized by partially laminated sediments, suggesting that recent conditions have been favoring
the preservation of these sediment structures. The presence of laminations in the uppermost parts of the cores, overlying a
homogeneous sediment, indicates that, at some point, monimolimnion was likely restricted to the deeper lake zones. Finally,
below a depth of 14 m, the lakebed is primarily anoxic and is almost exclusively occupied by well-preserved laminated
sediments. This demonstrates that oxygen conditions control laminae preservation, providing evidence for the past extent of
250 the hypolimnion.



5.2 Geochemical focusing

The chemical composition of the surface sediments of Lake Łazduny varies with lithological type and water depth. Spatial variability and GAMs (Fig. 7) indicate differences between homogenous and laminated sediments (Fig. A4). In the littoral zone, a mixture of minerogenic (Ti) and organic (TOC, TS) sediments dominate while sediments enriched in Fe and Mn dominate in deeper parts of the lake bottom, most probably as a result of geochemical focusing (Engstrom et al., 1985). The concurrence of organic and terrestrial matter is most probably a result of a broad littoral zone. Lake Łazduny cuts into the outwash plain sands and gravels, and small gullies developed in the glacial drift supply the shallow waters with terrestrial matter. Sparse mineral grains of the larger fractions were found in the sediments. Organic matter in Lake Łazduny has two major sources. Primary production leads to a uniform distribution of organic matter, which can then be concentrated in the basin's deepest parts. However, the shoreline of Lake Łazduny is densely vegetated. Deciduous trees are a source of litter that locally provides large quantities of organic matter, primarily carbon (DeGasparro et al., 2019) and nutrients, and sulfur (Hongve, 1999) to the littoral. Abundant Chara meadows, especially in the lake's northernmost part, provide an additional source of organic matter.

Fe_{org} is correlated with biogenic silica, consistent with its organic provenance, as Fe is an important nutrient and a constituent of diatom cells (Hutchins and Bruland, 1998). BSi, resulting mainly from the deposition of redox-resistant diatom valves (Smol and Stoermer, 2010), follows the expected pattern of focusing, with the highest concentrations in the deepest areas. Interestingly, most of the Fe is not correlated with sulfur concentrations. Only Fe_{org} shows a moderate correlation with S, suggesting that sulfide formation is not an important pathway for Fe. Interestingly, sulfur is deposited mainly in shallow areas, which are more often oxidized than deep sediments, suggesting deposition and cycling of organic-bound S (Couture et al., 2016). In the deeper parts of the lake elevated abundances of both Fe and Mn (oxy)hydroxides, which act as oxidizing agents, can be regarded as a occasional drivers of sulfur release (Urban, 1994). Furthermore, Charophyta meadows in the lake reside close to the shoreline, providing an additional source of algal organic matter and inducing calcite ($CaCO_3$) precipitation. This could explain higher TIC concentrations in the shallow lake zones rather than in the lake's deepest points. Manganese shows spatial patterns similar to those of iron (Fig. 5 and 6). However, the majority of Mn lies between the deposition of calcium-dominated carbonates and Fe-bearing matter (Fig. A3). Opposite trends in Mn concentrations relative to organic and terrestrial matter suggest that geochemical processes control manganese concentrations in sediments. Opposite signs in PC2 (Fig. A3) indicate that manganese concentrations peak while organic matter concentrations decline. The decomposition of organic matter is a well-known process that alters water pH and CO_2 availability, creating a pathway for carbonate formation. Mn and Fe carbonates in lacustrine settings are most often reported in varved sediments. Recent studies show that these carbonates are a plausible pathway for manganese burial in sediments of anoxic hypolimnion and are controlled by Mn availability or pH changes (Bonk et al., 2021; Dräger et al., 2017; Müller et al., 2021). High-resolution observations and sedimentological studies from Lake Żabiński have shown that rhodochrosite ($MnCO_3$) can constitute up to 15% of the annual mineral mass in the sediments (Żarczyński et al., 2022). This represents the intrinsic connection



285 between seasonal changes in the redox conditions that control the formation of these minerals (Davison et al., 1982) and the preservation of the varves (Zolitschka et al., 2015).

Mn and Fe carbonates and their dependence on water column stratification have also been reported in numerous marine settings (Astakhov et al., 2006; Burke and Kemp, 2002; Frederichs et al., 2003). Meister et al. (2009) suggest that the presence of Mn-oxides and their partial reduction during H₂S oxidation increases alkalinity and promotes the precipitation of Ca-rhodochrosite at geochemical focusing sites. This could also influence low sulfur concentrations in the deepest sediments of Lake Łazduny. Häusler et al. (2018) demonstrated that periods of deep-water oxygenation trap dissolved Mn in the reducing sediments, thereby facilitating carbonate formation. A diagnostic feature of the laminations of Lake Łazduny is autochthonous calcite (Tylmann et al., 2013b). Organic matter decomposition and elevated HCO₃⁻ supplied by calcite dissolution can lead to supersaturation of the sediment-water interface with respect to the Mn-carbonates (Stevens et al., 2000). Contact of the carbonate-rich surface waters with the Mn-enriched bottom waters was suggested early on (Dean and Megard, 1993) as a driving of Mn-carbonate formation. In Lake Ohnuma, rhodochrosite is associated with summer stratification and organic-rich lamina as a product of the Mn ions reacting with the HCO₃⁻ (Katsuta et al., 2020).

Yet, in mesotrophic Lake Łazduny primary production is a relatively low (Szczerba et al., 2021). Therefore, the decomposition of organic matter in sediments, the release of CO₂, and pH changes are less notable than in more productive lakes. Furthermore, Mn in Lake Łazduny sediments is deposited mainly as (oxy)hydroxides. Undoubtedly, the formation and preservation of Mn-bearing minerals in sediments is a complex problem that depends on water ventilation and pH (Jouve et al., 2013), as well as on the presence of organic matter and other minerals (Wittkop et al., 2020).

5.3. Contemporary variability of Fe and Mn versus their use as paleoredox proxies

The iron and manganese phases change with redox conditions and pH (Davison, 1993; Davison et al., 1982). As a result, Fe and Mn have been widely used in paleolimnological studies as paleoredox tracers, with the expectation that higher Fe and Mn concentrations reflect greater oxygen availability (Engstrom et al., 1985; Mackereth, 1966; Vegas-Vilarrúbia et al., 2018). However, other processes often control their abundance and spatial differentiation, such as delivery rates and provenance (Tribovillard et al., 2006) or biogeochemical cycling (Klaveness, 1977). Therefore, the interpretation of Fe and Mn in geological records requires caution (Tribovillard et al., 2006) and controlling for detrital delivery. This is achieved through elemental ratios, considering inert elements such as Ti (Kylander et al., 2011) or by testing multivariate relationships between the terrestrial inputs and trace metal abundances (Żarczyński et al., 2019). In Lake Łazduny, Ti_{clr} shows low importance in the dataset, whereas K_{clr} is either uncorrelated or anticorrelated with Fe and Mn (Fig. A3, Fig. 4). Therefore, we interpret Fe and Mn concentrations as diagnostic of at least partially redox-dependent processes. Our monitoring data, especially the depth of the oxycline and spatial Mn patterns, suggest a strong link between lake turnover, hypolimnetic oxygenation, and Mn burial in sediments.

315 As the oxycline migrates deeper into the water column, reductive dissolution and reoxidation processes increase the concentrations of Mn and Fe in the water and sediments (Fig. 8, Davison, 1993). Fe and Mn mobilization and migration



toward the deepest point depend partially on the development of anoxic conditions (Engstrom et al., 1985). Remobilized and geochemically focused, Fe and Mn are trapped in the hypolimnion and immobilized by short oxidation pulses. Sediment trap and core studies from Elk Lake suggest that (oxy)hydroxide could form during the mixing as oxycline migrates downwards, whereas (oxy)hydroxide rains occur likely during the stratification periods as redissolved Mn and Fe migrate upwards, possibly redistributing the Mn and Fe to the shallower depths (Nuhfer et al., 1993). Primarily, Fe (oxy)hydroxides are known to withstand anoxia to some extent and form semi-stable deposits (Dean and Megard, 1993; Żarczyński et al., 2019). Thus, geochemical focusing, coupled with rapid oxidation, can immobilize Fe and Mn in sediments. These, in turn, can act as electron acceptors during the oxidation of the other sediment components.

Scholtysik et al. (2020) showcased continuous sedimentation of Mn oxides throughout the summer and enrichment in the anoxic hypolimnion of Lake Stechlin. That kind of Mn behavior can lead to an interpretation of Mn (and Fe) profiles in the lake sediments that is contrary to the majority of the paleolimnological studies. Żarczyński et al. (2022) used Mn deposition events to accurately pinpoint holomixis in Lake Żabińskie, as Mn had to be first enriched in a seasonally anoxic environment. Even when Fe and Mn are remobilized in the anoxic hypolimnion, lake stratification hinders their possible loss via outflow, as, depending on lake morphology, dissolved Fe and Mn would have to cross the oxycline threshold and be mostly flushed out.

However, it must be stressed that the stratigraphic position of Fe and Mn enrichments must be accounted for. In Lake Łazduny once spatial variability is accounted for, a weak tendency for increased Fe and Mn burial in the deeper zones is visible, even though some of the deepest samples from Lake Łazduny exhibited a slightly lower Fe/Mn ratio, typically suggesting higher redox (Naeher et al., 2013). However, on longer scales, minuscule variability within the anoxic zone should not play an important role. A study of Sanchini et al. (2020) based on μ XRF, sedimentary pigments, and hyperspectral imaging provides independent evidence that, since its formation ca. 9750 cal BP, Lake Łazduny has experienced periods of either stable meromixis or seasonal anoxia, punctuated by mixing events. The former, especially over the last ca. 400 years, is linked to elevated Mn burial in sediments (Sanchini et al., 2020), driven by intensified lake mixing, supporting our interpretation. Yet, even during these periods of increased mixing intensity, Lake Łazduny remained seasonally anoxic. Therefore, we interpret mixing as a process leading to increased geochemical focusing. Our findings based on the uppermost sediments of Lake Łazduny suggest that even though seasonal anoxia is necessary for Fe and Mn enrichment and their geochemical focusing, these elements can be successfully used as proxies of past oxygenation of bottom water. In this sense, anoxia should be seen as a starting point which ultimately could lead to permanent Fe and Mn burial in the sediments once they become oxidized (Żarczyński et al., 2019).

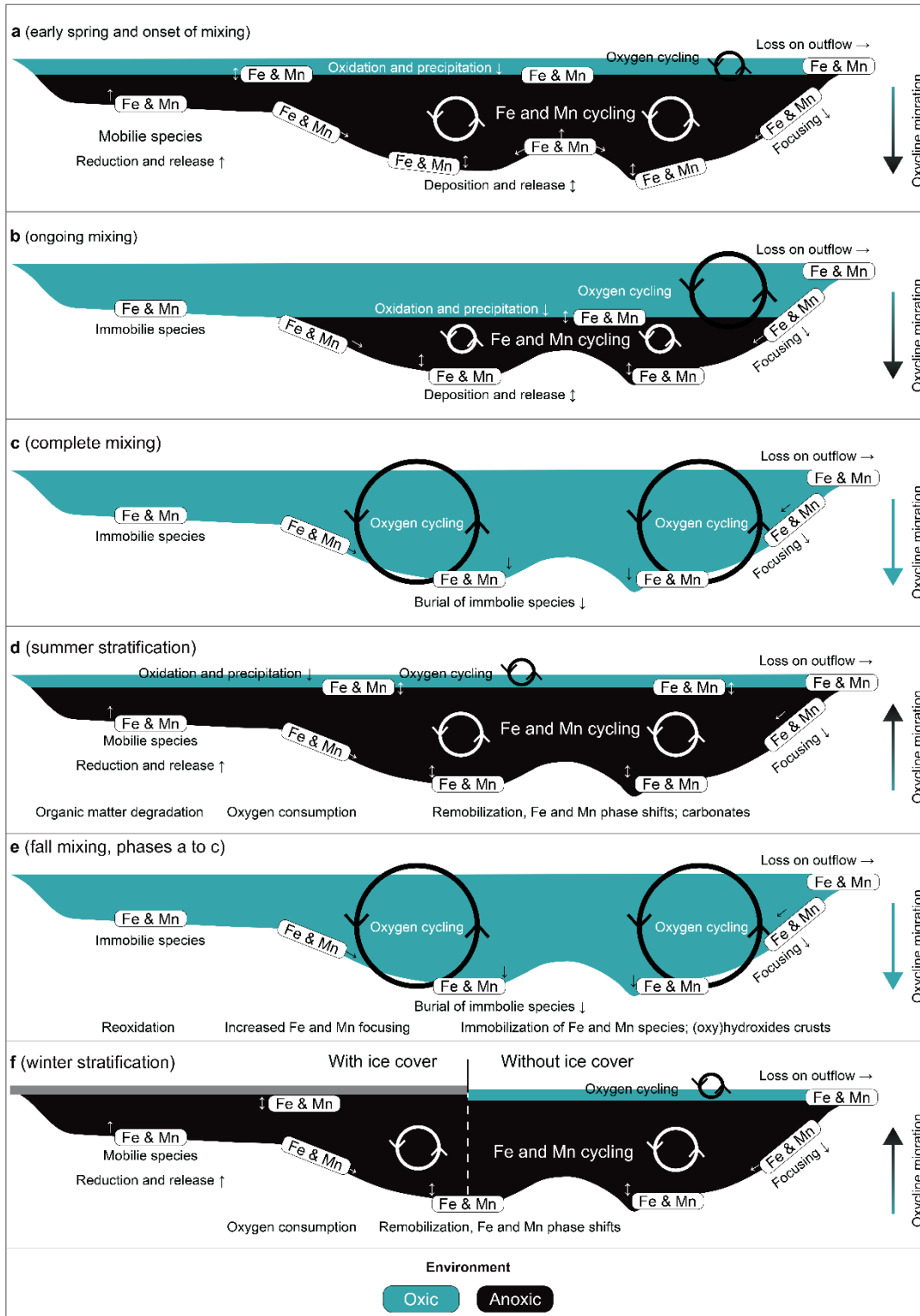




Figure 8: Schematic of mixing-driven geochemical Fe and Mn focusing in the Lake Łazduny.

6 Conclusions

Recognition of past water ventilation relies on numerous geochemical and sedimentological methods, including trace metals (Fe, Mn). However, the use of trace metals requires an understanding of the processes that control their spatial variability and mobility, and how these influence their fate in sediments. To better understand these complex relations, we analyzed modern limnological conditions in a small, relatively deep lake and focused on water temperature and dissolved oxygen concentrations to characterize the recent sedimentation environment. Then, we analyzed the spatial variability of sediment structure, bulk properties, elemental composition, and Fe and Mn fractions, relating this variability to sediment location and establishing a limnological framework, particularly regarding water-sediment interface oxygenation. Finally, we attempted to test whether iron and manganese concentrations differ significantly between sediment types under typical oxygen conditions.

We demonstrated that the spatial variation in Fe and Mn, and their burial, were mainly controlled by geochemical focusing, which, in turn, influenced the Fe/Mn ratio, a well-known paleoredox proxy. We found that the concentrations of Fe and Mn corresponded to lithological variability of the sediments, which in turn was related to prevailing redox conditions on the lake bottom. Furthermore, our data indicate that, despite complex interpretation, Fe, Mn, and their ratio are viable proxies of past redox changes. Additionally, using independent analytical methods, we demonstrated the high reliability of non-destructive techniques, such as μ XRF, in complex geochemical landscapes, including lacustrine sedimentary settings. Finally, further work should focus on the downcore variability of the tested elements and their application in a spatiotemporal context to trace lake evolution.

7 Code and data availability

The dataset, including water properties, ice cover presence, sedimentological and geochemical variables, is available from the Bridge of Knowledge – Open Research Data Catalog: <https://doi.org/10.34808/yak2-7w44>

8 Author contributions

MŻ: Conceptualization, Formal analysis, Investigation, Writing – original draft and final text, Visualization. **WT:** Resources, Writing – review & editing, Project administration, Funding acquisition, Supervision, Resources. **DE:** Resources, Writing – review & editing. **BSz:** Resources, Writing – review & editing.



9 Acknowledgements

We want to thank Jolanta Walkusz-Miotk, Christian Ohlendorf, Ksenia Pazdro, Anna Poraj-Górska, Sabine Stahl, and Bernd
375 Zolitschka for their assistance.

10 Financial support

This research is supported by the Polish Ministry of Science and Higher Education project NN306 275635.

11 References

- 380 Astakhov, A. S., Tiedemann, R., Murdmaa, I. O., Bogdanova, O. Yu., Mozherovsky, A. V., and Sereda, N. A.: Manganese carbonates in the upper quaternary sediments of the Deryugin basin (Sea of Okhotsk), *Oceanology*, 46, 716–729, <https://doi.org/10.1134/S0001437006050122>, 2006.
- Bertrand, S., Tjallingii, R., Kylander, M. E., Wilhelm, B., Roberts, S. J., Arnaud, F., Brown, E., and Bindler, R.: Inorganic geochemistry of lake sediments: A review of analytical techniques and guidelines for data interpretation, *Earth-Science Reviews*, 249, 104639, <https://doi.org/10.1016/j.earscirev.2023.104639>, 2024.
- 385 Boehrer, B., von Rohden, C., and Schultze, M.: Physical Features of Meromictic Lakes: Stratification and Circulation, in: *Ecology of Meromictic Lakes*, vol. 228, edited by: Gulati, R. D., Zadereev, E. S., and Degermendzhi, A. G., Springer International Publishing, Cham, 15–34, https://doi.org/10.1007/978-3-319-49143-1_2, 2017.
- 390 Bonk, A., Tylmann, W., Amann, B., Enters, D., and Grosjean, M.: Modern limnology, sediment accumulation and varve formation processes in Lake Żabińskie, northeastern Poland: comprehensive process studies as a key to understand the sediment record, *J Limnol*, 74, 358–370, <https://doi.org/10.4081/jlimnol.2014.1117>, 2015.
- Bonk, A., Müller, D., Ramisch, A., Kramkowski, M. A., Noryśkiewicz, A. M., Sekudewicz, I., Gąsiorowski, M., Luberd-Durnaś, K., Słowiński, M., Schwab, M., Tjallingii, R., Brauer, A., and Błaszczewicz, M.: Varve microfacies and chronology from a new sediment record of Lake Gościąż (Poland), *Quaternary Science Reviews*, 251, 106715, <https://doi.org/10.1016/j.quascirev.2020.106715>, 2021.
- 395 Burke, I. T. and Kemp, A. E. S.: Microfabric analysis of Mn-carbonate laminae deposition and Mn-sulfide formation in the Gotland Deep, Baltic Sea, *Geochimica et Cosmochimica Acta*, 66, 1589–1600, [https://doi.org/10.1016/S0016-7037\(01\)00860-2](https://doi.org/10.1016/S0016-7037(01)00860-2), 2002.
- Couture, R.-M., Fischer, R., Van Cappellen, P., and Gobeil, C.: Non-steady state diagenesis of organic and inorganic sulfur in lake sediments, *Geochimica et Cosmochimica Acta*, 194, 15–33, <https://doi.org/10.1016/j.gca.2016.08.029>, 2016.
- 400 Davison, W.: Iron and manganese in lakes, *Earth-Science Reviews*, 34, 119–163, [https://doi.org/10.1016/0012-8252\(93\)90029-7](https://doi.org/10.1016/0012-8252(93)90029-7), 1993.
- Davison, W., Woof, C., and Rigg, E.: The dynamics of iron and manganese in a seasonally anoxic lake; direct measurement of fluxes using sediment traps, *Limnology and Oceanography*, 27, 987–1003, <https://doi.org/10.4319/lo.1982.27.6.0987>, 1982.



- 405 Dean, W. E. and Megard, R. O.: Environment of deposition of CaCO₃ in Elk Lake, Minnesota, in: Geological Society of America Special Papers, vol. 276, Geological Society of America, 97–114, <https://doi.org/10.1130/SPE276-p97>, 1993.
- DeGasparro, S. D., Beresford, D. V., Prater, C., and Frost, P. C.: Leaf litter decomposition in boreal lakes: variable mass loss and nutrient release ratios across a geographic gradient, *Hydrobiologia*, <https://doi.org/10.1007/s10750-019-04140-w>, 2019.
- 410 Dräger, N., Theuerkauf, M., Szeroczyńska, K., Wulf, S., Tjallingii, R., Plessen, B., Kienel, U., and Brauer, A.: Varve microfacies and varve preservation record of climate change and human impact for the last 6000 years at Lake Tiefer See (NE Germany), *The Holocene*, 27, 450–464, <https://doi.org/10.1177/0959683616660173>, 2017.
- Dresti, C., Rogora, M., and Fenocchi, A.: Hypolimnetic oxygen depletion in a deep oligomictic lake under climate change, *Aquat Sci*, 85, 4, <https://doi.org/10.1007/s00027-022-00902-2>, 2022.
- 415 Engstrom, D. R. and Wright, H. E. J.: Chemical stratigraphy of lake sediments as a record of environmental change, in: *Lake Sediments and Environmental History.*, edited by: Haworth, E. Y. and Lund, J. W. G., Leicester University Press, 11–67, 1984.
- Engstrom, D. R., Swain, E. B., and Kingston, J. C.: A palaeolimnological record of human disturbance from Harvey’s Lake, Vermont: geochemistry, pigments and diatoms, *Freshwater Biology*, 15, 261–288, <https://doi.org/10.1111/j.1365-2427.1985.tb00200.x>, 1985.
- 420 Filzmoser, P., Fritz, H., and Kalcher, K.: *pcaPP: Robust PCA by Projection Pursuit*, , GitHub.com, 2024.
- Frederichs, T., von Dobeneck, T., Bleil, U., and Dekkers, M. J.: Towards the identification of siderite, rhodochrosite, and vivianite in sediments by their low-temperature magnetic properties, *Physics and Chemistry of the Earth, Parts A/B/C*, 28, 669–679, [https://doi.org/10.1016/S1474-7065\(03\)00121-9](https://doi.org/10.1016/S1474-7065(03)00121-9), 2003.
- 425 Häusler, K., Dellwig, O., Schnetger, B., Feldens, P., Leipe, T., Moros, M., Pollehne, F., Schönke, M., Wegwerth, A., and Arz, H. W.: Massive Mn carbonate formation in the Landsort Deep (Baltic Sea): Hydrographic conditions, temporal succession, and Mn budget calculations, *Marine Geology*, 395, 260–270, <https://doi.org/10.1016/j.margeo.2017.10.010>, 2018.
- 430 He, W., You, L., Chen, M., Tuo, Y., Liao, N., Wang, H., and Li, J.: Varied sediment archive of Fe and Mn contents under changing reservoir mixing patterns, oxygenation regimes, and runoff inputs, *Ecological Indicators*, 147, 109967, <https://doi.org/10.1016/j.ecolind.2023.109967>, 2023.
- Hongve, D.: Production of dissolved organic carbon in forested catchments, *Journal of Hydrology*, 224, 91–99, [https://doi.org/10.1016/S0022-1694\(99\)00132-8](https://doi.org/10.1016/S0022-1694(99)00132-8), 1999.
- 435 Hounshell, A. G., McClure, R. P., Lofton, M. E., and Carey, C. C.: Whole-ecosystem oxygenation experiments reveal substantially greater hypolimnetic methane concentrations in reservoirs during anoxia, *Limnol Oceanogr*, 6, 33–42, <https://doi.org/10.1002/lol2.10173>, 2021.
- Hutchins, D. A. and Bruland, K. W.: Iron-limited diatom growth and Si:N uptake ratios in a coastal upwelling regime, *Nature*, 393, 561–564, <https://doi.org/10.1038/31203>, 1998.
- Hutorowicz, H., Grabowska, K., and Nowicka, A.: Charakterystyka warunków klimatycznych Pojezierza Mazurskiego, *Zeszyty Problemowe Postępów Nauk Rolniczych*, 431, 21–29, 1996.



- 440 Jane, S. F., Hansen, G. J. A., Kraemer, B. M., Leavitt, P. R., Mincer, J. L., North, R. L., Pilla, R. M., Stetler, J. T., Williamson, C. E., Woolway, R. I., Arvola, L., Chandra, S., DeGasperi, C. L., Diemer, L., Dunalska, J., Erina, O., Flaim, G., Grossart, H.-P., Hambright, K. D., Hein, C., Hejzlar, J., Janus, L. L., Jenny, J.-P., Jones, J. R., Knoll, L. B., Leoni, B., Mackay, E., Matsuzaki, S.-I. S., McBride, C., Müller-Navarra, D. C., Paterson, A. M., Pierson, D., Rogora, M., Rusak, J. A., Sadro, S., Saulnier-Talbot, E., Schmid, M., Sommaruga, R., Thiery, W., Verburg, P., Weathers, K. C., Weyhenmeyer, G. A.,
445 Yokota, K., and Rose, K. C.: Widespread deoxygenation of temperate lakes, *Nature*, 594, 66–70, <https://doi.org/10.1038/s41586-021-03550-y>, 2021.

Jenny, J.-P., Francus, P., Normandeau, A., Lapointe, F., Perga, M.-E., Ojala, A., Schimmelmann, A., and Zolitschka, B.: Global spread of hypoxia in freshwater ecosystems during the last three centuries is caused by rising local human pressure, *Glob Change Biol*, 22, 1481–1489, <https://doi.org/10.1111/gcb.13193>, 2016a.

- 450 Jenny, J.-P., Normandeau, A., Francus, P., Taranu, Z. E., Gregory-Eaves, I., Lapointe, F., Jautzy, J., Ojala, A. E. K., Dorioz, J.-M., Schimmelmann, A., and Zolitschka, B.: Urban point sources of nutrients were the leading cause for the historical spread of hypoxia across European lakes, *Proc Natl Acad Sci USA*, 113, 12655–12660, <https://doi.org/10.1073/pnas.1605480113>, 2016b.

- Jouve, G., Francus, P., Lamoureux, S., Provencher-Nolet, L., Hahn, A., Haberzettl, T., Fortin, D., and Nuttin, L.:
455 Microsedimentological characterization using image analysis and μ -XRF as indicators of sedimentary processes and climate changes during Lateglacial at Laguna Potrok Aike, Santa Cruz, Argentina, *Quaternary Science Reviews*, 71, 191–204, <https://doi.org/10.1016/j.quascirev.2012.06.003>, 2013.

- Katsuta, N., Naito, S., Ikeda, H., Tanaka, K., Murakami, T., Ochiai, S., Miyata, Y., Shimizu, M., Hayano, A., Fukui, K., Hasegawa, H., Nagao, S., Nakagawa, M., Nagashima, K., Niwa, M., Murayama, M., Kagawa, M., and Kawakami, S.:
460 Sedimentary rhythm of Mn-carbonate laminae induced by East Asian summer monsoon variability and human activity in Lake Ohnuma, southwest Hokkaido, northern Japan, *Quaternary Science Reviews*, 248, 106576, <https://doi.org/10.1016/j.quascirev.2020.106576>, 2020.

Klaveness, D.: Morphology, distribution and significance of the manganese-accumulating microorganism metallogenium in lakes, *Hydrobiologia*, 56, 25–33, <https://doi.org/10.1007/BF00023282>, 1977.

- 465 Kylander, M. E., Ampel, L., Wohlfarth, B., and Veres, D.: High-resolution X-ray fluorescence core scanning analysis of Les Echets (France) sedimentary sequence: new insights from chemical proxies, *J. Quaternary Sci.*, 26, 109–117, <https://doi.org/10.1002/jqs.1438>, 2011.

- Li, J., Molot, L. A., Palmer, M. E., Winter, J. G., Young, J. D., and Stainsby, E. A.: Long-term changes in hypolimnetic dissolved oxygen in a large lake: Effects of invasive mussels, eutrophication and climate change on Lake Simcoe, 1980–
470 2012, *Journal of Great Lakes Research*, 44, 779–787, <https://doi.org/10.1016/j.jglr.2018.05.016>, 2018.

Mackereth, F. J. H.: Some chemical observations on post-glacial lake sediments, *Phil. Trans. R. Soc. Lond. B*, 250, 165–213, <https://doi.org/10.1098/rstb.1966.0001>, 1966.

- Marks, L., Dzierżek, J., Janiszewski, R., Kaczorowski, J., Lindner, L., Majecka, A., Makos, M., Szymanek, M., Tołoczko-Pasek, A., and Woronko, B.: Quaternary stratigraphy and palaeogeography of Poland, *Acta Geologica Polonica*, 66, 410–
475 434, <https://doi.org/10.1515/agp-2016-0018>, 2016.

Meister, P., Bernasconi, S. M., Aiello, I. W., Vasconcelos, C., and McKenzie, J. A.: Depth and controls of Ca-rhodochrosite precipitation in bioturbated sediments of the Eastern Equatorial Pacific, ODP Leg 201, Site 1226 and DSDP Leg 68, Site 503, *Sedimentology*, 56, 1552–1568, <https://doi.org/10.1111/j.1365-3091.2008.01046.x>, 2009.



- 480 Müller, D., Tjallingii, R., Płóciennik, M., Luoto, T. P., Kotrys, B., Plessen, B., Ramisch, A., Schwab, M. J., Błaszkiwicz, M., Słowiński, M., and Brauer, A.: New insights into lake responses to rapid climate change: the Younger Dryas in Lake Gościąż, central Poland, *Boreas*, 50, 535–555, <https://doi.org/10.1111/bor.12499>, 2021.
- Müller, P. J. and Schneider, R.: An automated leaching method for the determination of opal in sediments and particulate matter, *Deep Sea Research Part I: Oceanographic Research Papers*, 40, 425–444, [https://doi.org/10.1016/0967-0637\(93\)90140-X](https://doi.org/10.1016/0967-0637(93)90140-X), 1993.
- 485 Naeher, S., Gilli, A., North, R. P., Hamann, Y., and Schubert, C. J.: Tracing bottom water oxygenation with sedimentary Mn/Fe ratios in Lake Zurich, Switzerland, *Chemical Geology*, 352, 125–133, <https://doi.org/10.1016/j.chemgeo.2013.06.006>, 2013.
- Nuhfer, E. B., Anderson, R. Y., Bradbury, J. P., and Dean, W. E.: Modern sedimentation in Elk Lake, Clearwater County, Minnesota, *Geological Society of America Special Papers*, 276, 75–96, <https://doi.org/10.1130/SPE276-p75>, 1993.
- 490 Nürnberg, G. K.: The Anoxic Factor, a Quantitative Measure of Anoxia and Fish Species Richness in Central Ontario Lakes, *Transactions of the American Fisheries Society*, 124, 677–686, [https://doi.org/10.1577/1548-8659\(1995\)124<0677:TAFAQM>2.3.CO;2](https://doi.org/10.1577/1548-8659(1995)124<0677:TAFAQM>2.3.CO;2), 1995.
- Nychka, D. and Furrer, R.: fields: Tools for spatial data, , GitHub.com, 2021.
- Ohlendorf, C.: A sample carrier for measuring discrete powdered samples with an ITRAX XRF core scanner, *X-Ray Spectrometry*, 47, 58–62, <https://doi.org/10.1002/xrs.2811>, 2018.
- Peterson, G. D., Beard, T. D., Beisner, B. E., Bennett, E. M., Carpenter, S. R., Cumming, G. S., Dent, C. L., and Havlicek, T. D.: Assessing Future Ecosystem Services: a Case Study of the Northern Highlands Lake District, Wisconsin, *Conservation Ecology*, 7, 2003.
- 500 Poraj-Górska, A. I., Bonk, A., Żarczyński, M., Kinder, M., and Tylmann, W.: Varved lake sediments as indicators of recent cultural eutrophication and hypolimnetic hypoxia in lakes, *Anthropocene*, 36, 100311, <https://doi.org/10.1016/j.ancene.2021.100311>, 2021.
- R Core Team: R: A language and environment for statistical computing, 2025.
- 505 Roeser, P., Dräger, N., Brykała, D., Ott, F., Pinkerneil, S., Gierszewski, P., Lindemann, C., Plessen, B., Brademann, B., Kaszubski, M., Fojutowski, M., Schwab, M. J., Słowiński, M., Błaszkiwicz, M., and Brauer, A.: Advances in understanding calcite varve formation: new insights from a dual lake monitoring approach in the southern Baltic lowlands, *Boreas*, 50, 419–440, <https://doi.org/10.1111/bor.12506>, 2021.
- Sanchini, A., Szidat, S., Tylmann, W., Vogel, H., Wacnik, A., and Grosjean, M.: A Holocene high-resolution record of aquatic productivity, seasonal anoxia and meromixis from varved sediments of Lake Łazduny, North-Eastern Poland: insight from a novel multi-proxy approach, *Journal of Quaternary Science*, 35, 1070–1080, <https://doi.org/10.1002/jqs.3242>, 2020.
- 510 Scholtysik, G., Dellwig, O., Roeser, P., Arz, H. W., Casper, P., Herzog, C., Goldhammer, T., and Hupfer, M.: Geochemical focusing and sequestration of manganese during eutrophication of Lake Stechlin (NE Germany), *Biogeochemistry*, 151, 313–334, <https://doi.org/10.1007/s10533-020-00729-9>, 2020.
- 515 Sirota, I., Tjallingii, R., Pinkerneil, S., Schroeder, B., Albert, M., Kearney, R., Heiri, O., Breu, S., and Brauer, A.: Tracing rate and extent of human-induced hypoxia during the last 200 years in the mesotrophic lake, Tiefer See (NE Germany), *Biogeosciences*, 21, 4317–4339, <https://doi.org/10.5194/bg-21-4317-2024>, 2024.



- Smol, J. P. and Stoermer, E. F. (Eds.): *The Diatoms: Applications for the Environmental and Earth Sciences*, 2nd ed., Cambridge University Press, Cambridge, <https://doi.org/10.1017/CBO9780511763175>, 2010.
- Stevens, L. R., Ito, E., and Olson, D. E. L.: Relationship of Mn-carbonates in varved lake-sediments to catchment vegetation in Big Watab Lake, MN, USA, *Journal of Paleolimnology*, 24, 199–211, 2000.
- 520 Szczerba, A., Pla-Rabes, S., Żarczyński, M., and Tylmann, W.: The relationship between chrysophyte cyst assemblages and meteorological conditions: Evidence from a sediment-trap study in northeast Poland, *Ecological Indicators*, 133, 108395, <https://doi.org/10.1016/j.ecolind.2021.108395>, 2021.
- Szczerba, A., Rzodkiewicz, M., and Tylmann, W.: Modern diatom assemblages and their association with meteorological conditions in two lakes in northeastern Poland, *Ecological Indicators*, 147, 110028, <https://doi.org/10.1016/j.ecolind.2023.110028>, 2023.
- 525 Templ, M., Hron, K., and Filzmoser, P.: robCompositions: an R-package for robust statistical analysis of compositional data, in: *Compositional Data Analysis. Theory and Applications*, edited by: Pawlowsky-Glahn, V. and Buccianti, A., John Wiley & Sons, Chichester (UK), 341–355, 2011.
- Tessier, A., Campbell, P. G. C., and Bisson, M.: Sequential extraction procedure for the speciation of particulate trace metals, *Anal. Chem.*, 51, 844–851, <https://doi.org/10.1021/ac50043a017>, 1979.
- 530 Tomczyk, A. M. and Bednorz, E.: *Atlas klimatu Polski (1991-2020)*, Bogucki Wydawnictwo Naukowe, Poznań, 2022.
- Tribouillard, N., Algeo, T. J., Lyons, T., and Riboulleau, A.: Trace metals as paleoredox and paleoproductivity proxies: An update, *Chemical Geology*, 232, 12–32, <https://doi.org/10.1016/j.chemgeo.2006.02.012>, 2006.
- Tylmann, W.: Pobór i opróbowanie powierzchniowych, silnie uwodnionych osadów jeziornych o nienaruszonej strukturze — uwagi metodyczne i stosowany sprzęt, 55, 2007.
- 535 Tylmann, W., Szpakowska, K., Ohlendorf, C., Woszczyk, M., and Zolitschka, B.: Conditions for deposition of annually laminated sediments in small meromictic lakes: a case study of Lake Suminko (northern Poland), *J Paleolimnol*, 47, 55–70, <https://doi.org/10.1007/s10933-011-9548-3>, 2012.
- Tylmann, W., Zolitschka, B., Enters, D., and Ohlendorf, C.: Laminated lake sediments in northeast Poland: distribution, preconditions for formation and potential for paleoenvironmental investigation, *J Paleolimnol*, 50, 487–503, <https://doi.org/10.1007/s10933-013-9741-7>, 2013a.
- 540 Tylmann, W., Enters, D., Kinder, M., Moska, P., Ohlendorf, C., Poręba, G., and Zolitschka, B.: Multiple dating of varved sediments from Lake Łazduny, northern Poland: Toward an improved chronology for the last 150 years, *Quaternary Geochronology*, 15, 98–107, <https://doi.org/10.1016/j.quageo.2012.10.001>, 2013b.
- 545 Tylmann, W., Głowacka, P., and Szczerba, A.: Tracking climate signals in varved lake sediments: research strategy and key sites for comprehensive process studies in the Masurian Lakeland, *Limnological Review*, 17, 159–166, <https://doi.org/10.1515/limre-2017-0015>, 2017.
- Urban, N. R.: Retention of Sulfur in Lake Sediments, in: *Environmental Chemistry of Lakes and Reservoirs*, vol. 237, edited by: Baker, L. A., American Chemical Society, Washington, DC, 323–369, <https://doi.org/10.1021/ba-1994-0237.ch010>, 1994.
- 550



Vegas-Vilarrúbia, T., Corella, J. P., Pérez-Zanón, N., Buchaca, T., Trapote, M. C., López, P., Sigró, J., and Rull, V.: Historical shifts in oxygenation regime as recorded in the laminated sediments of lake Montcortès (Central Pyrenees) support hypoxia as a continental-scale phenomenon, *Science of The Total Environment*, 612, 1577–1592, <https://doi.org/10.1016/j.scitotenv.2017.08.148>, 2018.

555 Wetzel, R. G.: Oxygen, in: *Limnology (Third Edition)*, edited by: Wetzel, R. G., Academic Press, San Diego, 151–168, <https://doi.org/10.1016/B978-0-08-057439-4.50013-7>, 2001.

Wickham, H., Averick, M., Bryan, J., Chang, W., McGowan, L., François, R., Grolemund, G., Hayes, A., Henry, L., Hester, J., Kuhn, M., Pedersen, T., Miller, E., Bache, S., Müller, K., Ooms, J., Robinson, D., Seidel, D., Spinu, V., Takahashi, K., Vaughan, D., Wilke, C., Woo, K., and Yutani, H.: Welcome to the Tidyverse, *JOSS*, 4, 1686, <https://doi.org/10.21105/joss.01686>, 2019.

Wittkop, C., Swanner, E. D., Grengs, A., Lambrecht, N., Fakhræe, M., Myrbo, A., Bray, A. W., Poulton, S. W., and Katsev, S.: Evaluating a primary carbonate pathway for manganese enrichments in reducing environments, *Earth and Planetary Science Letters*, 538, 116201, <https://doi.org/10.1016/j.epsl.2020.116201>, 2020.

Wood, S.: *mgcv: Mixed GAM Computation Vehicle with Automatic Smoothness Estimation*, 2019.

565 Woolway, R. I. and Merchant, C. J.: Worldwide alteration of lake mixing regimes in response to climate change, *Nature Geoscience*, 12, 271–276, <https://doi.org/10.1038/s41561-019-0322-x>, 2019.

Yuan, L. L. and Jones, J. R.: Modeling hypolimnetic dissolved oxygen depletion using monitoring data, *Can. J. Fish. Aquat. Sci.*, 77, 814–823, <https://doi.org/10.1139/cjfas-2019-0294>, 2020.

570 Żarczyński, M., Wacnik, A., and Tylmann, W.: Tracing lake mixing and oxygenation regime using the Fe/Mn ratio in varved sediments: 2000 year-long record of human-induced changes from Lake Żabińskie (NE Poland), *Science of The Total Environment*, 657, 585–596, <https://doi.org/10.1016/j.scitotenv.2018.12.078>, 2019.

Żarczyński, M., Zander, P. D., Grosjean, M., and Tylmann, W.: Linking the formation of varves in a eutrophic temperate lake to meteorological conditions and water column dynamics, *Science of The Total Environment*, 842, 156787, <https://doi.org/10.1016/j.scitotenv.2022.156787>, 2022.

575 Zimmerman, A. J. and Weindorf, D. C.: Heavy Metal and Trace Metal Analysis in Soil by Sequential Extraction: A Review of Procedures, *International Journal of Analytical Chemistry*, 2010, 387803, <https://doi.org/10.1155/2010/387803>, 2010.

Zolitschka, B., Francus, P., Ojala, A. E. K., and Schimmelmann, A.: Varves in lake sediments – a review, *Quaternary Science Reviews*, 117, 1–41, <https://doi.org/10.1016/j.quascirev.2015.03.019>, 2015.

Appendix A

580 Methods

Fe and Mn sequential extraction

The homogenized sediment samples were weighed into Teflon® tubes. Four subsequent solutions were prepared for each sample; the solution of surface-bound ions (A): 25 cm³ of acetic acid (CH₃COOH) was added to 500 cm³ of ultrapure water, then topped to 1000 cm³. After that, the solution was diluted four times to C = 0.11 mol dm⁻³. Solution of (oxy)hydroxides



585 (B): 6.95 g of hydroxylamine hydrochloride ($\text{NH}^2\text{OH}\cdot\text{HCl}$) dissolved in 900 cm^3 ultrapure water and acidified with nitric acid (HNO_3) to pH 2 and topped to 1000 cm^3 . Solution of organic matter-bound ions (C): Hydrogen peroxide (H_2O_2) 8.8 mol dm^{-3} . And solution of ions within the siliciclastic minerals lattices (D): 77.1 g ammonium acetate ($\text{CH}_3\text{COONH}_4$) dissolved in 900 cm^3 ultrapure water, acidified to pH 2 with HNO_3 , and topped to 1000 cm^3 . Hydrofluoric acid (HF) and 0.1 mol dm^{-3} , and HNO_3 were also used. Merck Suprapur grade reagents were used at all stages of analysis. After each step, samples were
 590 centrifuged at 3500 RPM for 15 min at 22 °C using a Megafuge (Thermo Fisher Scientific) centrifuge and then decanted. An air–acetylene flame was used during the procedure, and a deuterium lamp was used for background correction.

Results

Table A1: Concentrations of the selected elemental variables in the sediments of Lake Łazduny grouped by sediment type (in %).

Variable	Laminated				Homogeneous			
	Mean	SD	Min	Max	Mean	SD	Min	Max
TOC	15.67	5.38	5.48	21.03	17.73	4.06	6.71	24.25
TN	1.56	0.52	0.58	2.10	1.83	0.47	0.69	2.75
TIC	4.48	1.66	2.42	8.12	5.10	1.30	2.67	8.27
TS	0.90	0.28	0.21	1.48	0.91	0.41	0.21	1.59
BSi	17.95	3.90	11.60	25.20	9.31	2.90	5.50	15.30

595 **Table A2:** Concentrations of the major Fe fractions in the sediments of Lake Łazduny grouped by sediment type (in $\mu\text{g g}^{-1}$).

Fraction	Laminated				Homogeneous			
	Mean	SD	Min	Max	Mean	SD	Min	Max
Fe _{surf}	29.71	24.72	7.00	83.00	9.88	7.04	3.00	33.00
Fe _{oxy}	44.57	48.17	8.00	157.00	14.12	12.55	4.00	55.00
Fe _{org}	1,137.43	556.88	406.00	2,093.00	590.38	372.98	71.00	1,403.00
Fe _{sil}	8,438.21	4,313.04	4,266.00	18,107.00	5,405.88	1,735.86	1,420.00	9,506.00
Fe _{tot}	9,649.93	4,118.08	4,776.00	19,010.00	6,020.25	1,891.26	1,505.00	9,837.00

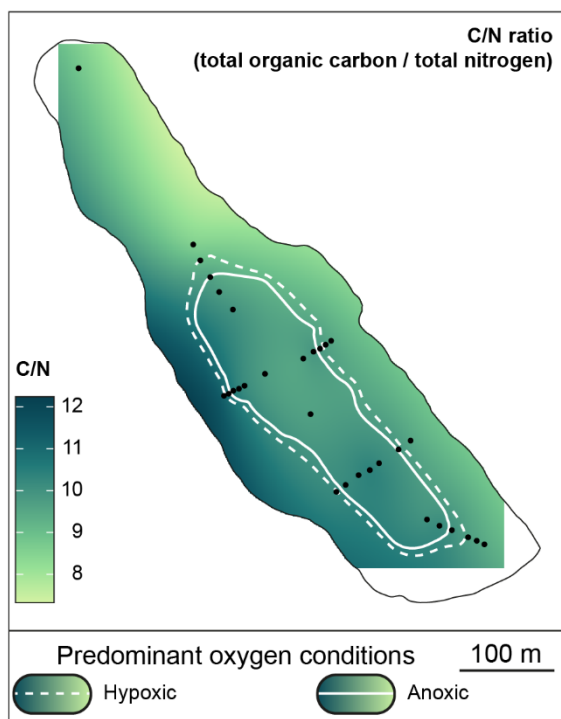


Table A3: Concentrations of the major Mn fractions in the sediments of Lake Łazduny grouped by sediment type (in $\mu\text{g g}^{-1}$).

Fraction	Laminated				Homogeneous			
	Mean	SD	Min	Max	Mean	SD	Min	Max
Mn_{surf}	179.07	58.61	100.00	276.00	136.00	40.43	63.00	192.00
Mn_{oxy}	165.14	199.00	35.00	647.00	68.69	46.94	186.00	36.00
Mn^{org}	156.29	68.36	85.00	315.00	123.62	59.93	49.00	320.00
Mn_{sil}	55.86	37.50	29.00	147.00	40.94	21.11	22.00	112.00
Mn_{tot}	556.36	327.94	264.00	1,385.00	369.25	137.35	201.00	745.00

Spatial C/N variability

The C/N ratio (total organic carbon to total nitrogen) showed a clear, expected pattern, with higher values near the western lake shore (Fig. A1). This is the steeper side of the tunnel channel, which is more prone to erosion and the delivery of detrital matter. In the extreme sense, it is evident from numerous fallen tree trunks occupying this zone, either due to land instability or activity by the European beaver (*Castor fiber*). The eastern shore, as well as the deepest lake parts, is depleted in terrestrial organic matter and may exhibit a spatial extent similar to that of BSi, with lower C/N ratios found in areas of higher BSi abundance.



605 **Figure A1:** Spatial variability of the C/N ratio in the sediments. Dots indicate coring locations.



Statistical relationships

Robust principal component analysis (RPCA) was visualized with “ggfortify” 0.4.18 (Tang et al., 2016). The first two principal components explained 36.68% and 15.97% of the total variance, respectively. Together, the first two components explained 52.65% of the variance in the dataset (Fig. A3). However, robust principal component analysis typically yields lower values than ordinary PCA, a trade-off for increased robustness (Żarczyński et al., 2019). Importantly, compared with Spearman’s correlation matrix, RPCA presents a slightly different picture because it relies on the median absolute deviation (MAD) to analyze multivariate datasets (Filzmoser et al., 2024). Overall, the PC1 separates samples from homogeneous and laminated sediments. Homogeneous sediments, found in the oxic zone, are better described by carbonate and detrital matter. In contrast, samples from laminated sediments are characterized by elevated concentrations of biogenic silica and trace metals. Variables representing organic matter (TN, TS, S_{clr}) were primarily correlated with the terrigenous input proxies (Ti_{clr} , K_{clr}). Together, these variables formed the first group. However, due to its reliance on the MAD in the PCA space, TOC was strongly correlated with Fe_{org} and Fe_{tot} . Except for Mn_{surf} , all the Mn species formed the second group, associated with lake depth. Fe had the most dispersion, with different fractions correlated with different variable groups. Fe_{sili} correlated weakly with carbonate content and tended to deviate toward shallow-water environments. Other fractions were primarily associated with the deeper, anoxic sediments. BSi and Si_{clr} were the most prominent variables driving the positive side of PC1, which was associated with the laminated sediments.

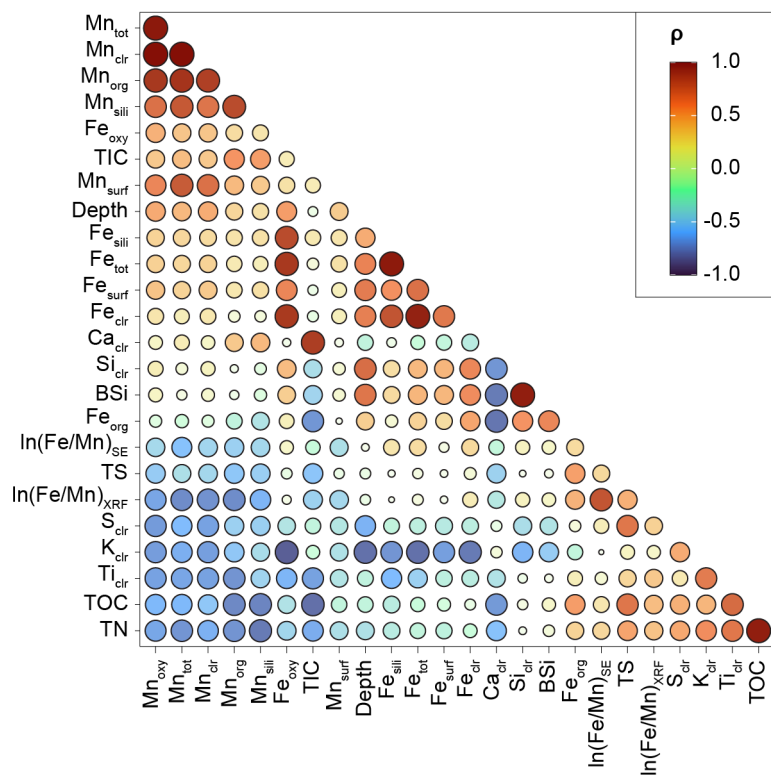


Figure A2: Correlations between selected elemental variables in Lake Łazduny sediments (Spearman's rank correlation).



625

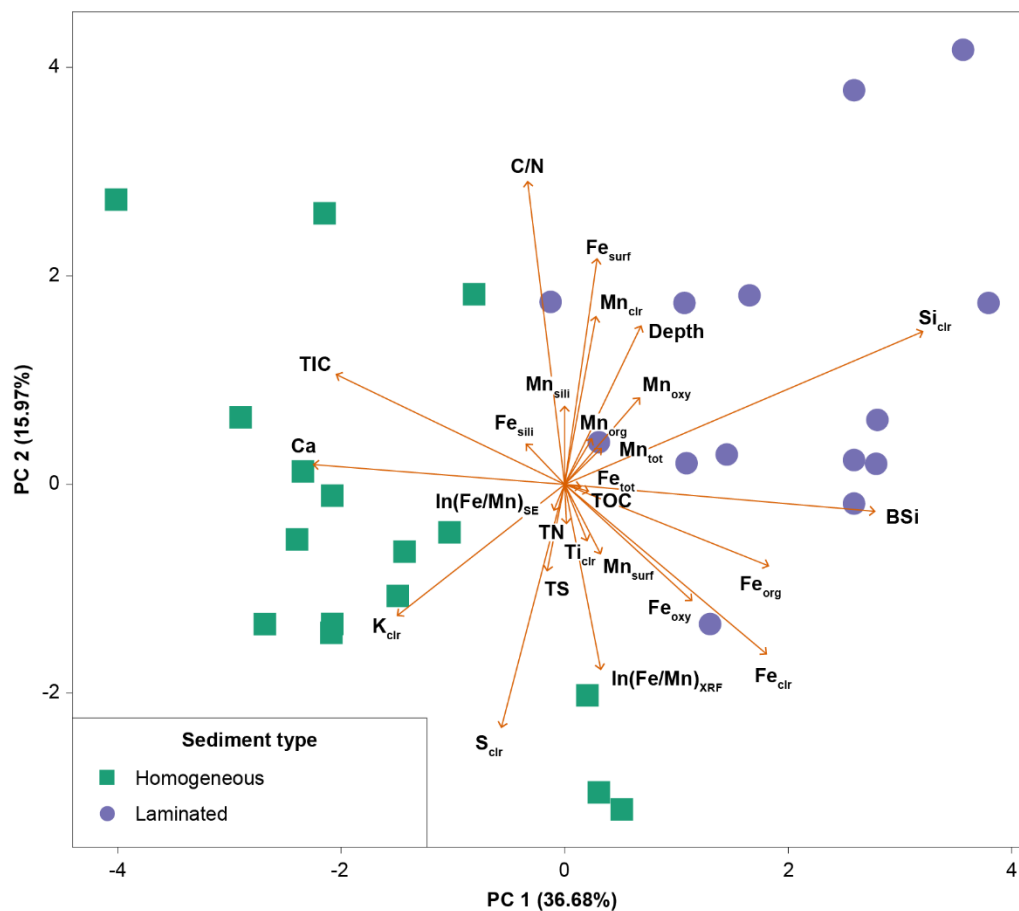
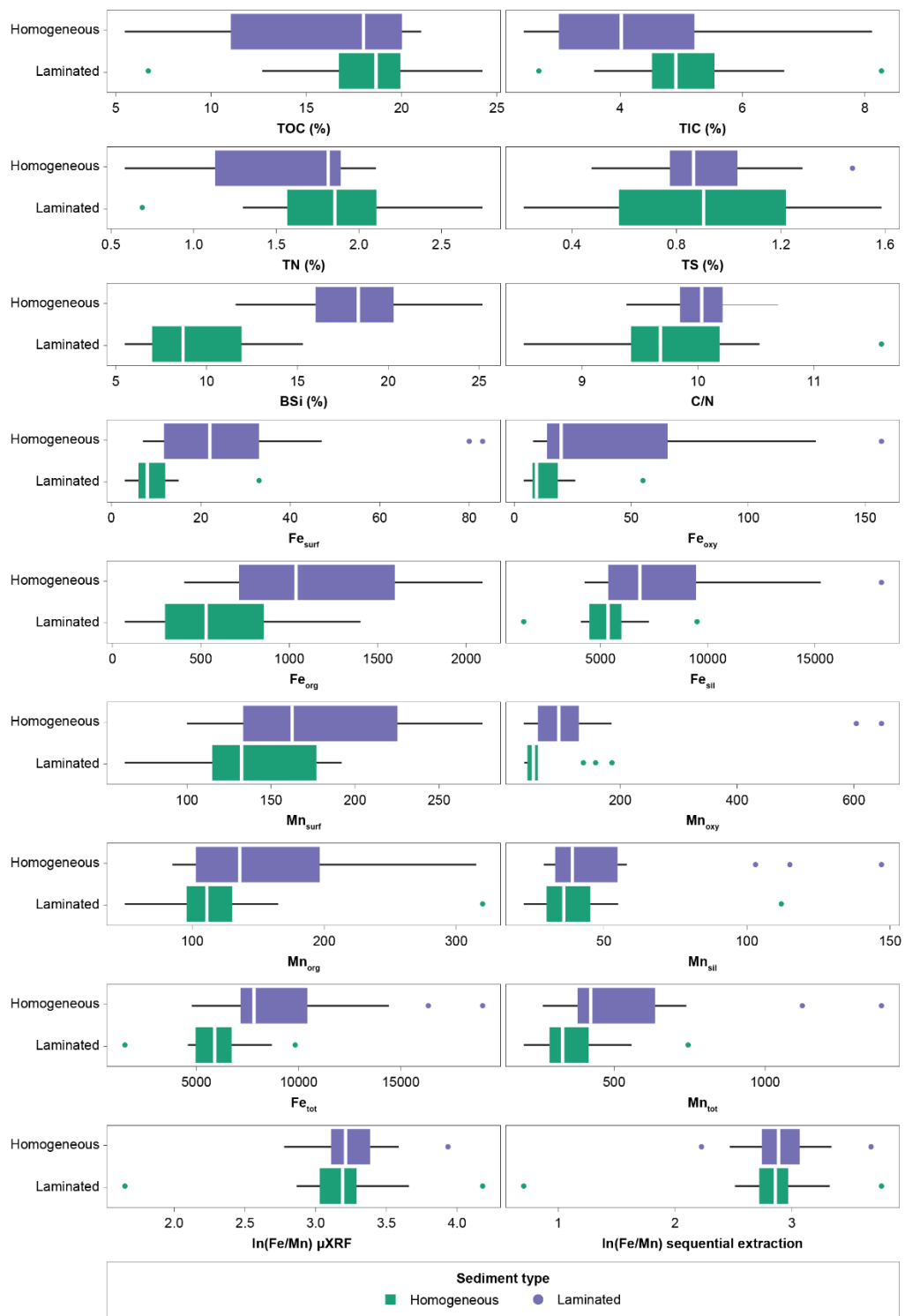


Figure A3: Robust principal component analysis biplot based on multivariable dataset from 30 surface samples. One sample was removed due to an error in the sequential extraction measurement.



630 **Figure A4: Boxplots of selected geochemical variables grouped by sediment type.**



Spatial Fe/Mn variability

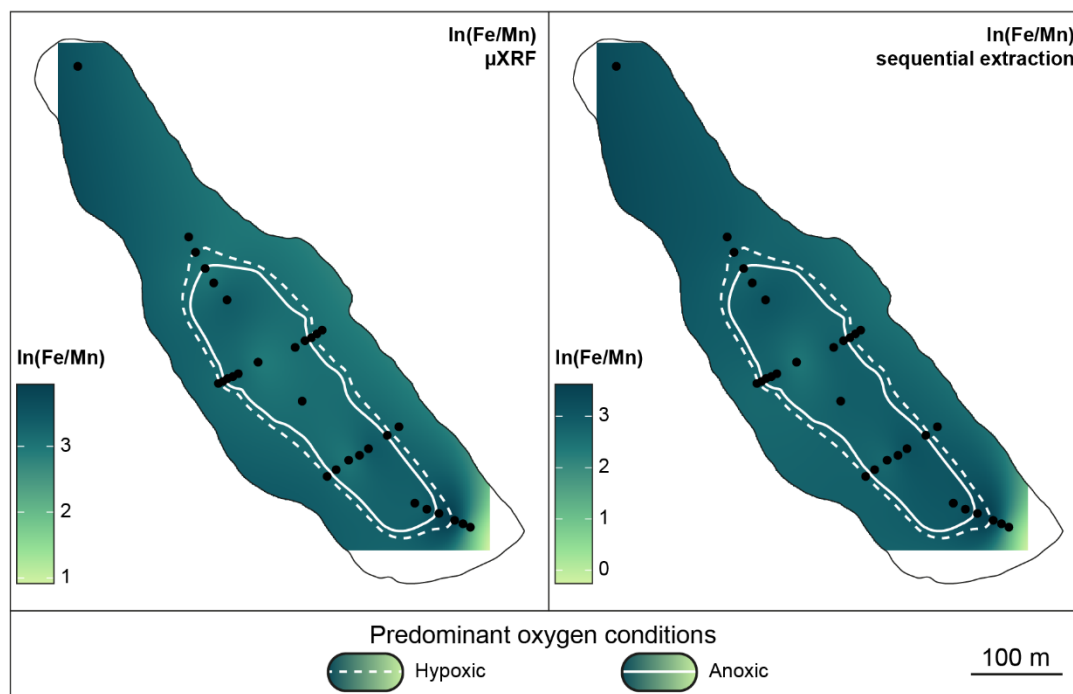


Figure A5: Spatial extent of the Fe/Mn ratio from μ XRF and sequential extraction measurements. Dots indicate coring locations.

References

- 635 Filzmoser, P., Fritz, H., and Kalcher, K.: pcaPP: Robust PCA by Projection Pursuit, , GitHub.com, 2024.
- Tang, Y., Horikoshi, M., and Li, W.: ggfortify: Unified Interface to Visualize Statistical Results of Popular R Packages, R J., 8, 474, <https://doi.org/10.32614/RJ-2016-060>, 2016.
- 640 Żarczyński, M., Wacnik, A., and Tylmann, W.: Tracing lake mixing and oxygenation regime using the Fe/Mn ratio in varved sediments: 2000 year-long record of human-induced changes from Lake Żabińskie (NE Poland), Sci. Total Environ., 657, 585–596, <https://doi.org/10.1016/j.scitotenv.2018.12.078>, 2019.